

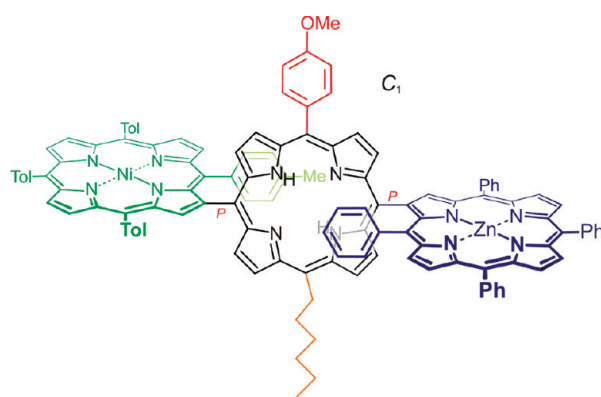
## Synthesis and Stereochemistry of Highly Unsymmetric $\beta$ ,*Meso*-Linked Porphyrin Arrays

Daniel C. G. Götz,<sup>†</sup> Torsten Bruhn,<sup>†</sup> Mathias O. Senge,<sup>\*,‡</sup> and Gerhard Bringmann<sup>\*,†</sup>

<sup>†</sup>*Institute of Organic Chemistry and Röntgen Research Center for Complex Material Systems, University of Würzburg, Am Hubland, D-97074 Würzburg, Germany, and* <sup>‡</sup>*School of Chemistry, SFI Tetrapyrrole Laboratory, Trinity College Dublin, Dublin 2, Ireland*

bringman@chemie.uni-wuerzburg.de; sengem@tcd.ie

Received July 10, 2009



Porphyrin arrays with tailor-made photophysical properties and well-defined three-dimensional geometries constitute attractive synthetic targets in porphyrin chemistry. The paper describes a variable, straightforward synthetic procedure for the construction of  $\beta$ ,*meso*-linked porphyrin multichromophores in good to excellent yields. In a Suzuki-type coupling reaction  $\beta$ -borylated 5,10,15,20-tetraarylporphyrins (TAPs) served as versatile building blocks for the preparation of a plethora of directly linked, unsymmetrically substituted di- and triporphyrins. Besides their interesting photophysical properties, especially the trimeric porphyrin arrays show exciting stereochemical features. The established protocols thus open a convenient entry into the synthesis of achiral and chiral, unsymmetrically substituted  $\beta$ ,*meso*-linked oligoporphyrins, e.g., for applications in biomedicine or nonlinear optics.

### Introduction

The synthesis and physicochemical characterization of oligomeric porphyrin assemblies has been the subject of intense research in recent years.<sup>1,2</sup> Porphyrin-derived multichromophores display unique physical and optical properties,<sup>3</sup>

reflecting the electronic “communication” between the monomeric subunits in the array, thus accounting for their potential applications in chemistry, biology, and physics.

In nature, tetrapyrroles, as the “pigments of life”,<sup>4</sup> play a number of crucial biological roles, such as, e.g., reaction catalysis, molecular binding, electron and energy transfer,

\*To whom correspondence should be addressed. (G.B.) Fax: +49 931 888 4755. Tel: +49 931 318 5323. (M.O.S.) Fax: +353 1 896 8536. Tel: +353 1 896 8537.

(1) (a) Burrell, A. K.; Officer, D. L.; Plieger, P. G.; Reid, D. C. W. *Chem. Rev.* **2001**, *101*, 2751–2796 and references cited therein. (b) Vicente, M. G. H.; Jaquinod, L.; Smith, K. M. *Chem. Commun.* **1999**, 1771–1782 and references cited therein.

(2) Iengo, E.; Zangrando, E.; Alessio, E. *Acc. Chem. Res.* **2006**, *39*, 841–851 and references cited therein.

(3) (a) Tsuda, A.; Furuta, H.; Osuka, A. *J. Am. Chem. Soc.* **2001**, *123*, 10304–10321. (b) Kim, D.; Osuka, A. *J. Phys. Chem. A* **2003**, *107*, 8791–8816. (c) Kim, D.; Osuka, A. *Acc. Chem. Res.* **2004**, *37*, 735–745. (d) Ikeue, T.; Furukawa, K.; Hata, H.; Aratani, N.; Shinokubo, H.; Kato, T.; Osuka, A. *Angew. Chem., Int. Ed.* **2005**, *44*, 6899–6901. (e) Ahn, T. K.; Kim, K. S.; Kim, D. Y.; Noh, S. B.; Aratani, N.; Ikeda, C.; Osuka, A.; Kim, D. *J. Am. Chem. Soc.* **2006**, *128*, 1700–1704.

(4) (a) Battersby, A. R. *Nat. Prod. Rep.* **1987**, *4*, 77–87. (b) Battersby, A. R. *Pure Appl. Chem.* **1993**, *65*, 1113–1122.

and light harvesting.<sup>5,6</sup> The importance and diversity of these functions has inspired many synthetically oriented groups to design artificial tetrapyrrole systems—among them porphyrin dimers, trimers, and oligomers with covalent linkages between the monomeric porphyrin subunits<sup>1,2</sup>—mimicking their natural counterparts.<sup>7–9</sup> As a consequence, oligoporphyrins have gained significant importance as substrates for molecular sensing<sup>10</sup> and

molecular recognition,<sup>11</sup> as catalysts in asymmetric synthesis,<sup>12</sup> for optical<sup>13</sup> or medical<sup>14</sup> applications, and as building blocks for the construction of molecular (nano)materials.<sup>15</sup>

Because of the rapidly increasing importance of these applications there is an urgent need for efficient, versatile, and straightforward procedures for the construction of unsymmetrically substituted porphyrin arrays with well-defined three-dimensional geometries and tailor-made chemical, physical, and optical properties. However, the synthesis of suitable assemblies of tetrapyrrole macrocycles is often time-consuming and requires the sometimes tedious multistep formation of adequately functionalized monomeric porphyrin precursors.<sup>1</sup>

According to the two types of reactive sites of a porphyrin ( $\beta$ - and *meso*-positions), porphyrin-derived multichromophores can be linked via three different types of direct

(5) Battersby, A. R. *Nat. Prod. Rep.* **2000**, *17*, 507–526 and references cited therein.

(6) *Tetrapyrroles: Birth, Life and Death (Molecular Biology Intelligence Unit)*; Warren, M. J., Smith, A. G., Eds.; Springer Verlag: New York, 2009 and references cited therein.

(7) For artificial tetrapyrrole systems used in reaction catalysis, see: (a) Collman, J. P.; Wagenknecht, P. S.; Hutchison, J. E. *Angew. Chem., Int. Ed. Engl.* **1994**, *33*, 1537–1554. (b) Ozaki, S. i.; Matsui, T.; Roach, M. P.; Watanabe, Y. *Coord. Chem. Rev.* **2000**, *198*, 39–59. (c) Vincente, M. G. H.; Smith, K. M. *Curr. Org. Chem.* **2000**, *4*, 139–174. (d) Vinhadó, F. S.; Martins, P. R.; Iamamoto, Y. *Curr. Top. Catal.* **2002**, *3*, 199–213. (e) Stephenson, N. A.; Bell, A. T. *J. Mol. Catal. A: Chem.* **2007**, *275*, 54–62. (f) Doyle, M. P. *Angew. Chem., Int. Ed.* **2009**, *48*, 850–852.

(8) For some recent examples of molecular binding properties of artificial porphyrin systems, see: (a) Zheng, J.-Y.; Konishi, K.; Aida, T. *Tetrahedron* **1997**, *53*, 9115–9122. (b) Weiss, J. *J. Inclusion Phenom. Macrocycl. Chem.* **2001**, *40*, 1–22. (c) Zhou, H.; Groves, J. T. *J. Porphyrins Phthalocyanines* **2004**, *8*, 125–140. (d) Mamardashvili, N. Z.; Maltseva, O. V.; Ivanova, Y. B.; Mamardashvili, G. M. *Tetrahedron Lett.* **2008**, *49*, 3752–3756. (e) Chekme-neva, E.; Hunter, C. A.; Packer, M. J.; Turega, S. M. *J. Am. Chem. Soc.* **2008**, *130*, 17718–17725. (f) Yang, J.; Cho, S.; Yoo, H.; Park, J.; Li, W.-S.; Aida, T.; Kim, D. *J. Phys. Chem. A* **2008**, *112*, 6869–6876. (g) Silva, I.; Sansone, S.; Brancalione, L. *Protein J.* **2009**, *28*, 1–13.

(9) For recent reviews on artificial photosynthetic model systems derived from porphyrins, see: (a) Wasielewski, M. R. *Chem. Rev.* **1992**, *92*, 435–461. (b) Gust, D.; Moore, T. A.; Moore, A. L. *Acc. Chem. Res.* **1993**, *26*, 198–205. (c) Gust, D.; Moore, T. A.; Moore, A. L. *Acc. Chem. Res.* **2001**, *34*, 40–48. (d) Fukuzumi, S.; Imahori, H. *Electron Transfer Chem.* **2001**, *2*, 927–975. (e) Imahori, H.; Mori, Y.; Matano, Y. *J. Photochem. Photobiol., C* **2003**, *4*, 51–83. (f) Guldi, D. M. *Chem. Soc. Rev.* **2002**, *31*, 22–36. (g) Kobuke, Y.; Ogawa, K. *Bull. Chem. Soc. Jpn.* **2003**, *76*, 689–708. (h) Imahori, H. *Org. Biomol. Chem.* **2004**, *2*, 1425–1433. (i) Imahori, H. *J. Phys. Chem. B* **2004**, *108*, 6130–6143. (j) Fukuzumi, S. *Bull. Chem. Soc. Jpn.* **2006**, *79*, 177–195. (k) Satake, A.; Kobuke, Y. *Org. Biomol. Chem.* **2007**, *5*, 1679–1691. (l) Hori, T.; Nakamura, Y.; Aratani, N.; Osuka, A. *J. Organomet. Chem.* **2007**, *692*, 148–155. (m) Jiang, L.; Li, Y. *J. Porphyrins Phthalocyanines* **2007**, *11*, 299–312. (n) Nakamura, Y.; Aratani, N.; Osuka, A. *Chem. Soc. Rev.* **2007**, *36*, 831–845.

(10) For selected recent examples of applications of porphyrins in molecular sensing, see: (a) Konishi, K.; Kimata, S.; Yoshida, K.; Tanaka, M.; Aida, T. *Angew. Chem., Int. Ed. Engl.* **1996**, *35*, 2823–2825. (b) Ashkenasy, G.; Ivanisevic, A.; Cohen, R.; Felder, C. E.; Cahen, D.; Ellis, A. B.; Shanzer, A. *J. Am. Chem. Soc.* **2000**, *122*, 1116–1122 ( $O_2$  sensing). (c) Doolling, C. M.; Worsfold, O.; Richardson, T. H.; Tregonning, R.; Vysotsky, M. O.; Hunter, C. A.; Kato, K.; Shinbo, K.; Kaneko, F. *J. Mater. Chem.* **2001**, *11*, 392–398 ( $NO_2$  sensing). (d) Zhang, X.-B.; Guo, C.-C.; Li, Z.-Z.; Shen, G.-L.; Yu, R.-Q. *Anal. Chem.* **2002**, *74*, 821–825 (sensing of mercury ions). (e) Kim, Y.-H.; Hong, J.-I. *Chem. Commun.* **2002**, 512–513 (sensing of NaCN). (f) Bucher, C.; Devillers, C. H.; Moutet, J.-C.; Royal, G.; Saint-Aman, E. *Chem. Commun.* **2003**, 888–889 (sensing of neutral molecules). (g) Zhang, Y.; Yang, R.; Liu, F.; Li, K. A. *Anal. Chem.* **2004**, *76*, 7336–7345 (imidazole sensing). (h) Niu, C.-G.; Gui, X.-Q.; Zeng, G.-M.; Guan, A.-L.; Gao, P.-F.; Qin, P.-Z. *Anal. Bioanal. Chem.* **2005**, *383*, 349–357 (pH sensing). (i) Zhang, H.; Sun, Y.; Ye, K.; Zhang, P.; Wang, Y. *J. Mater. Chem.* **2005**, *15*, 3181–3186 ( $O_2$  sensing). (j) Kejik, Z.; Zaruba, K.; Michalik, D.; Sebek, J.; Dian, J.; Pataridis, S.; Volka, K.; Kral, V. *Chem. Commun.* **2006**, 1533–1535 (sensing of ATP). (k) Gulino, A.; Mineo, P.; Scamporrino, E.; Vitalini, D.; Fragala, I. *Chem. Mater.* **2006**, *18*, 2404–2410 (pH sensing). (l) Xie, Y.; Hill, J. P.; Charvet, R.; Ariga, K. *J. Nanosci. Nanotechnol.* **2007**, *7*, 2969–2993. (m) Shoji, Y.; Tashiro, K.; Aida, T. *Chirality* **2008**, *20*, 420–424.

(11) For reviews on porphyrins used for chiral recognition, see: (a) Ogoshi, H.; Mizutani, T. *Acc. Chem. Res.* **1998**, *31*, 81–89. (b) Huang, X.; Nakanishi, K.; Berova, N. *Chirality* **2000**, *12*, 237–255. (c) Simonneaux, G.; Le Maux, P. *Coord. Chem. Rev.* **2002**, *228*, 43–60.

(12) For selected examples of porphyrins used in asymmetric synthesis, see: (a) Collman, J. P.; Zhang, X.; Lee, V. J.; Uffelman, E. S.; Brauman, J. I. *Science* **1993**, *261*, 1404–1411. (b) Gross, Z.; Ini, S. *J. Org. Chem.* **1997**, *62*, 5514–5521. (c) Rose, E.; Quelquejeu, M.; Pandian, R. P.; Lécas-Nawrocka, A.; Vilar, A.; Ricart, G.; Collman, J. P.; Wang, Z.; Straumanis, A. *Polyhedron* **2000**, *19*, 581–586. (d) Zhang, J.-L.; Zhou, H.-B.; Huang, J.-S.; Che, C.-M. *Chem.—Eur. J.* **2002**, *8*, 1554–1562. (e) Ferrand, Y.; Le Maux, P.; Simonneaux, G. *Org. Lett.* **2004**, *6*, 3211–3214. (f) Zhang, R.; Yu, W.-Y.; Che, C.-M. *Tetrahedron: Asymmetry* **2005**, *16*, 3520–3526.

(13) Data storage: (a) Ao, R.; Kummerl, L.; Haarer, D. *Adv. Mater.* **1995**, *7*, 495. Nonlinear optics: (b) Nalwa, H. S. *Adv. Mater.* **1993**, *5*, 341. Electrochromism: (c) Mortimer, R. J. *Chem. Soc. Rev.* **1997**, *26*, 147. Optical limiting: (d) Perry, J. W.; Mansour, K.; Lee, I.-Y. S.; Wu, X.-L.; Bedworth, P. V.; Chen, C.-T.; Ng, D.; Marder, S. R.; Miles, P.; Wada, T.; Tian, M.; Sasabe, H. *Science* **1996**, *273*, 1533.

(14) Photodynamic therapy (PDT): (a) Moan, J. *Photochem. Photobiol.* **1986**, *43*, 681. (b) Dougherty, T. J. *Adv. Photochem.* **1992**, *17*, 275–311. (c) Dougherty, T. J.; Marcus, S. L. *Eur. J. Cancer* **1992**, *28*, 1734–1742. (d) Bonnett, R. *Chem. Soc. Rev.* **1995**, *24*, 19–33. (e) Franck, B.; Nonn, A. *Angew. Chem., Int. Ed. Engl.* **1995**, *34*, 1795–1811. (f) Sternberg, E. D.; Dolphin, D. *Tetrahedron* **1998**, *54*, 4151–4202. (g) MacDonald, I. J.; Dougherty, T. J. *J. Porphyrins Phthalocyanines* **2001**, *5*, 105–129. Boron neutron capture therapy (BNCT): (h) Barth, R. F.; Soloway, A. H.; Brugger, R. M. *Cancer Invest.* **1996**, *14*, 534–550. (i) Kahl, S. B.; Li, J. *Inorg. Chem.* **1996**, *35*, 3878. (j) Soloway, A. H.; Tjarks, W.; Barnum, B. A.; Rong, F.-G.; Barth, R. F.; Codogni, I. M.; Wilson, J. G. *Chem. Rev.* **1998**, *98*, 1515–1562. DNA cleavage: (k) An, J. M.; Yang, S. J.; Yi, S.-Y.; Jhon, G.-J.; Nam, W. *Bull. Korean Chem. Soc.* **1997**, *18*, 117. (l) Mehta, G.; Muthusamy, S.; Maiya, B. G.; Arounaguirri, S. *Tetrahedron Lett.* **1997**, *38*, 7125. (m) Barth, R. F.; Coderre, J. A.; Vicente, M. G. H.; Blue, T. E. *Clin. Cancer Res.* **2005**, *11*, 3987–4002.

(15) For some recent examples, see: (a) Crossley, M. J.; Burn, P. L. *J. Chem. Soc., Chem. Commun.* **1991**, 1569. (b) Wagner, R. W.; Lindsey, J. S. *J. Am. Chem. Soc.* **1994**, *116*, 9759. (c) Wagner, R. W.; Lindsey, J. S.; Seth, J.; Palaniappan, V.; Bocian, D. F. *J. Am. Chem. Soc.* **1996**, *118*, 3996. (d) Harth, E. M.; Hecht, S.; Helms, B.; Malmstrom, E. E.; Frechet, J. M. J.; Hawker, C. J. *J. Am. Chem. Soc.* **2002**, *124*, 3926–3938. (e) Murakami, H.; Nomura, T.; Nakashima, N. *Chem. Phys. Lett.* **2003**, *378*, 481–485. (f) Tsuda, M.; Dy, E. S.; Kasai, H. *Eur. Phys. J. D* **2006**, *38*, 139–141. (g) Elemans, J. A. A. W.; van Hameren, R.; Nolte, R. J. M.; Rowan, A. E. *Adv. Mater.* **2006**, *18*, 1251–1266 and references cited therein. (h) Fukuzumi, S.; Kojima, T. *J. Mater. Chem.* **2008**, *18*, 1427–1439.

(16) Osuka, A.; Shimidzu, H. *Angew. Chem., Int. Ed. Engl.* **1997**, *36*, 135–137. (17) Yoshida, N.; Osuka, A. *Tetrahedron Lett.* **2000**, *41*, 9287–9291.

(18) (a) Susumu, K.; Shimidzu, T.; Tanaka, K.; Segawa, H. *Tetrahedron Lett.* **1996**, *37*, 8399–8402. (b) Senge, M. O.; Feng, X. *Tetrahedron Lett.* **1999**, *40*, 4165–4168. (c) Wojaczynski, J.; Latos-Grazynski, L.; Chmielewski, P. J.; Van Calcar, P.; Balch, A. L. *Inorg. Chem.* **1999**, *38*, 3040–3050. (d) Senge, M. O.; Feng, X. *J. Chem. Soc., Perkin Trans. 1* **2000**, 3615–3621. (e) Miller, M. A.; Lamm, R. K.; Prathapan, S.; Holten, D.; Lindsey, J. S. *J. Org. Chem.* **2000**, *65*, 6634–6649. (f) Hiroto, S.; Osuka, A. *J. Org. Chem.* **2005**, *70*, 4054–4058. (g) Jin, L.-M.; Chen, L.; Yin, J.-J.; Guo, C.-C.; Chen, Q.-Y. *Eur. J. Org. Chem.* **2005**, 3994–4001. (h) Jin, L.-M.; Yin, J.-J.; Chen, L.; Guo, C.-C.; Chen, Q.-Y. *Synlett* **2005**, 2893–2898.

(19) Aratani, N.; Osuka, A. *Org. Lett.* **2001**, *3*, 4213–4216.

(20) Khoury, R. C.; Jaquinod, L.; Smith, K. M. *Chem. Commun.* **1997**, 1057–1058.

(21) For directly *meso,meso*-linked dimmers derived from corrolid systems, see: Sankar, J.; Rath, H.; Prabhuraja, V.; Gokulnath, S.; Chandrashekar, T. K.; Purohit, C. S.; Verma, S. *Chem.—Eur. J.* **2007**, *13*, 105–114.

(22) (a) Bringmann, G.; Götz, D. C. G.; Gulder, T. A. M.; Gehrke, T. H.; Bruhn, T.; Kupfer, T.; Radacki, K.; Braunschweig, H.; Heckmann, A.; Lambert, C. *J. Am. Chem. Soc.* **2008**, *130*, 17812–17825. (b) Bringmann, G.; Rüdener, S.; Götz, D. C. G.; Gulder, T. A. M.; Reichert, M. *Org. Lett.* **2006**, *8*, 4743–4746.

(23) For  $\beta,\beta'$ -bisporphyrins without *meso*-substituents that might be axially chiral but have not been stereochemically characterized, see refs 24 and 25.

(24) Deng, Y.; Chang, C. K.; Nocera, D. G. *Angew. Chem., Int. Ed.* **2000**, *39*, 1066–1068.

(25) (a) Paine, J. B. III; Dolphin, D. *Can. J. Chem.* **1978**, *56*, 1710–1712. (b) Uno, H.; Kitawaki, Y.; Ono, N. *Chem. Commun.* **2002**, 116–117.

porphyrin–porphyrin connections: *meso,meso'*-,<sup>16–21</sup>  $\beta,\beta'$ -,<sup>22–27</sup> or  $\beta,meso$ .<sup>28–30</sup> The relative energies of the frontier orbitals—and, thus, also the electron transfer (ET) characteristics of such systems—are influenced by the chosen substituents of the porphyrin backbone and, in particular, by the type of the porphyrin–porphyrin linkage.<sup>31</sup> Thus, e.g., to gain detailed insight into the interplay of the monomeric subunits in directly linked porphyrin arrays in dependence of their connectivities, the availability of suitable porphyrin systems with different types of linkages and tunable electronic and optical properties is required.

Osuka and co-workers have pioneered the chemistry of *meso,meso'*-linked porphyrin arrays (Figure 1) by greatly facilitating the synthesis of such systems by introducing their AgPF<sub>6</sub>-promoted coupling protocol.<sup>16</sup> This procedure is, however, restricted to the preparation of oligomeric porphyrins arising from a homocoupling of two (or more) constitutionally identical precursors.<sup>32,33</sup> While *meso*-substituted porphyrin building blocks are usually available more easily by methods developed by Senge et al.,<sup>34</sup> viz. by regioselective nucleophilic addition of organolithium reagents to *meso*-unsubstituted porphyrin precursors and oxidation of the Meisenheimer-type intermediates, the synthesis of oligoporphyrins with direct  $\beta$ -linkages has, for a long time, been hampered by the lack of suitably  $\beta$ -functionalized tetraarylporphyrins (TAPs). Bringmann et al. have, therefore, recently established the synthesis of  $\beta$ -borylated TAPs from their respective brominated precursors by using a Miyaura-like transmetalation reaction.<sup>22</sup> The synthesized porphyrinyl boronic acid esters have proven to be valuable coupling partners in Suzuki couplings leading to the synthesis of a broad variety of intrinsically axially chiral

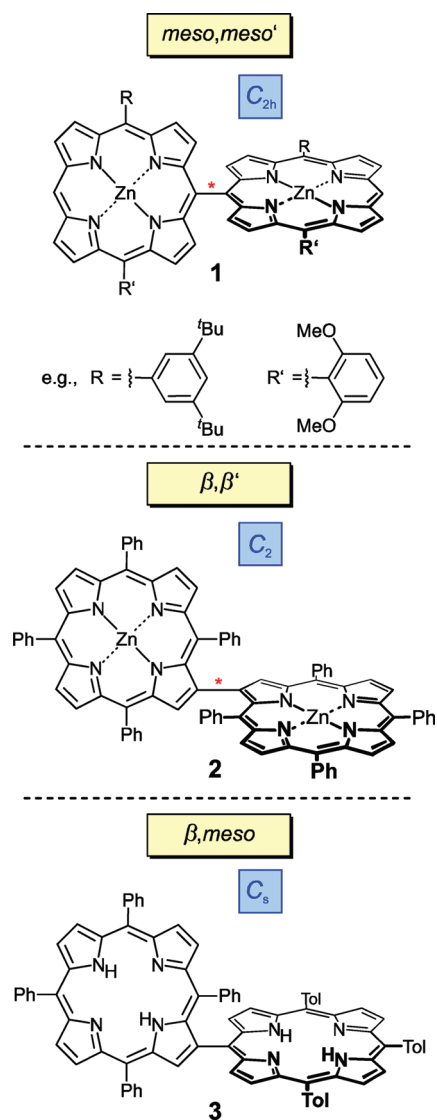


**FIGURE 1.** *Meso,meso'*-linked dimeric porphyrins **1**, whose axial chirality originates from their unsymmetric *meso*-substitution pattern as synthesized by Osuka et al.,<sup>17</sup>  $C_2$ -symmetric and thus intrinsically chiral  $\beta,\beta'$ -bisporphyrins of type **2** reported by Bringmann's group,<sup>22</sup> and one of the few literature-known representatives of (basically achiral)  $\beta,meso$ -linked porphyrin dimers **3** (Senge et al.).<sup>28</sup>

$\beta,\beta'$ -linked bisporphyrins (Figure 1). Although a few representatives of  $\beta,meso$ -linked porphyrin dimers or trimers have been synthesized,<sup>35</sup> no methodological study has so far aimed at the preparation of unsymmetric, directly  $\beta,meso$ -linked porphyrin arrays (Figure 1).

In this paper, we report on the synthesis of a variety of  $\beta,meso$ -linked porphyrin multichromophores via simple convergent reaction sequences in high yields, including dimeric and trimeric porphyrin arrays with axial chirality. The novel porphyrin trimers show interesting spectral and chiroptical properties and, in particular, possess unique

(26) For a directly  $\beta,\beta'$ -linked, yet *N*-confused bisporphyrin, which has been stereochemically characterized more recently, see: (a) Siczek, M.; Chmielewski, P. J. *Angew. Chem., Int. Ed.* **2007**, *46*, 7432–7436. For its synthesis, see: (b) Chmielewski, P. J. *Angew. Chem., Int. Ed.* **2004**, *43*, 5655–5658.

(27) For the synthesis and detailed characterization of directly  $\beta,\beta'$ -linked *corrole* dimers, see: (a) Mahammed, A.; Giladi, I.; Goldberg, I.; Gross, Z. *Chem.—Eur. J.* **2001**, *7*, 4259–4265. (b) Luobeznova, I.; Simkhovich, L.; Goldberg, I.; Gross, Z. *Eur. J. Inorg. Chem.* **2004**, 1724–1732. (c) Hiroto, S.; Furukawa, K.; Shinokubo, H.; Osuka, A. *J. Am. Chem. Soc.* **2006**, *128*, 12380–12381. (d) Barata, J. F. B.; Silva, A. M. G.; Neves, M. G. P. M. S.; Tomé, A. C.; Silva, A. M. S.; Cavaleiro, J. A. S. *Tetrahedron Lett.* **2006**, *47*, 8171–8174. (e) Cho, S.; Lim, J. M.; Hiroto, S.; Kim, P.; Shinokubo, H.; Osuka, A.; Kim, D. *J. Am. Chem. Soc.* **2009**, *131*, 6412–6420.

(28) (a) Wiehe, A.; Senge, M. O.; Schäfer, A.; Speck, M.; Tannert, S.; Kurreck, H.; Röder, B. *Tetrahedron* **2001**, *57*, 10089–10110. (b) Senge, M. O.; Rössler, B.; von Gersdorff, J.; Schäfer, A.; Kurreck, H. *Tetrahedron Lett.* **2004**, *45*, 3363–3367.

(29) (a) Wasielewski, M. R.; Johnson, D. G.; Niemczyk, M. P.; Gaines, G. L. III; O'Neil, M. P.; Svec, W. A. *J. Am. Chem. Soc.* **1990**, *112*, 6482–6488. (b) Johnson, D. G.; Niemczyk, M. P.; Minsek, D. W.; Wiederrecht, G. P.; Svec, W. A.; Gaines, G. L. III; Wasielewski, M. R. *J. Am. Chem. Soc.* **1993**, *115*, 5692–5701. (c) Zheng, G.; Pandey, R. K.; Forsyth, T. P.; Kozayev, A. N.; Dougherty, T. J.; Smith, K. M. *Tetrahedron Lett.* **1997**, *38*, 2409–2412.

(30) Ogawa, T.; Nishimoto, Y.; Yoshida, N.; Ono, N.; Osuka, A. *Angew. Chem., Int. Ed.* **1999**, *38*, 176–179.

(31) (a) Yang, S. I.; Seth, J.; Balasubramanian, T.; Kim, D.; Lindsey, J. S.; Holten, D.; Bocian, D. F. *J. Am. Chem. Soc.* **1999**, *121*, 4008–4018. (b) Huber, M. *Eur. J. Org. Chem.* **2001**, 4379–4389.

(32) For statistical AgPF<sub>6</sub>-promoted *meso,meso*-couplings between two different porphyrins, see: (a) Wojaczynski, J.; Lotos-Grazynski, L.; Chmielewski, P. J.; Calcar, P. V.; Balch, A. L. *Inorg. Chem.* **1999**, *38*, 3040. (b) Miller, M. A.; Lammi, R. K.; Prathapan, S.; Holten, D.; Lindsey, J. S. *J. Org. Chem.* **2000**, *65*, 6634.

(33) For a more general synthesis of *meso,meso*-linked bisporphyrins by Suzuki coupling reactions, see ref 19.

(34) (a) Feng, X.; Senge, M. O. *Tetrahedron* **2000**, *56*, 587–590. (b) Senge, M. O.; Bischoff, I. *Eur. J. Org. Chem.* **2001**, 1735–1751. (c) Ryppa, C.; Senge, M. O.; Hatscher, S. S.; Kleinpeter, E.; Wacker, P.; Schilde, U.; Wiehe, A. *Chem.—Eur. J.* **2005**, *11*, 3427–3442. (d) Senge, M. O. *Acc. Chem. Res.* **2005**, *38*, 733–743.

(35) (a) For the synthesis of  $\beta,meso$ -linked porphyrin dimers or trimers by mixed condensation reactions, see ref 28. (b) For the synthesis of similar  $\beta,meso$ -linked porphyrin-chlorin dyads and triads by mixed condensation reactions, see ref 29. (c) For the synthesis of  $\beta,meso$ -linked bisporphyrins by electrochemical oxidation of metalated porphyrins, see ref 30.

TABLE 1. Classification of Dimeric and Trimeric  $\beta$ ,*Meso*-Linked Porphyrins by the “ABCD Nomenclature”

substitution pattern	denotation
$R^1 = R^2 = R^3 =$ substituent 1	$A_3$ - $\beta$ TAP type
$R^1 = R^3 =$ substituent 1, $R^2 = H$	5,15- $A_2$ - $\beta$ TAP type
$R^1 = R^3 =$ substituent 1, $R^2 =$ substituent 2	5,15- $A_2B$ - $\beta$ TAP type
$R^1 =$ substituent 1, $R^3 =$ substituent 2, $R^2 = H$	5,15- $AB$ - $\beta$ TAP type
$R^1 =$ substituent 1, $R^2 =$ substituent 2, $R^3 =$ substituent 3	ABC- $\beta$ TAP type
$R^1 = R^3 =$ substituent 1, $R^2 =$ tetraarylporphyrin	$\beta$ TAP-5,15- $A_2$ - $\beta$ TAP' type
$R^1 =$ substituent 1, $R^3 =$ substituent 2; $R^2 =$ tetraarylporphyrin	$\beta$ TAP-5,15- $AB$ - $\beta$ TAP' type

stereochemical features. The established protocols open a convenient entry into the design of achiral and chiral, unsymmetrically substituted  $\beta$ ,*meso*-linked oligoporphyrins, e.g., for applications in biomedicine or nonlinear optics.

## Results and Discussion

**Classification of Unsymmetric  $\beta$ ,*Meso*-Linked Oligoporphyrins.** Besides the IUPAC nomenclature for tetrapyrrolic macrocycles,<sup>36</sup> another more practical denotation for *meso*-substituted porphyrins was proposed by Lindsey<sup>37</sup> to classify monomeric porphyrins by their different *meso*-substitution patterns. This nomenclature was further developed by Senge et al. and is now known as the ABCD system.<sup>34</sup> In order to facilitate the classification of the unsymmetrically substituted oligoporphyrins synthesized in the present work, we further extended the ABCD system to the unambiguous denotation of dimeric and trimeric  $\beta$ ,*meso*-linked porphyrins as shown in Table 1.

**Synthesis of  $\beta$ ,*Meso*-Linked Bisporphyrins.** The synthesis of  $\beta$ ,*meso*-linked dimeric porphyrins started with the Suzuki coupling<sup>38</sup> of suitable *meso*-brominated 5,15-di- or 5,10,15-trisubstituted porphyrins with  $\beta$ -borylated TAPs.<sup>22</sup> The respective brominated precursors were easily accessible by simple condensation reactions of dipyrromethanes with aldehydes<sup>39</sup> and subsequent functionalization of the generated 5,15-disubstituted porphyrins by addition of organolithium reagents,<sup>34</sup> followed by bromination according to

literature procedures.<sup>40</sup> The desired  $\beta$ -boronic acid esters of TAPs were synthesized by the Miyaura-like transmetalation protocol recently published.<sup>22</sup> Using the coupling conditions previously optimized for the synthesis of  $\beta$ , $\beta'$ -linked bisporphyrins,<sup>22</sup> a broad variety of  $\beta$ ,*meso*-linked porphyrin dimers were obtained in yields ranging from 50 up to 84% (Table 2).

Starting with 5,10,15-homosubstituted precursors and porphyrin boronic acid esters as the coupling partners, the simple  $C_s$ -symmetric  $A_3$ - $\beta$ TAP-type bisporphyrins **6a–d** bearing three identical aryl or alkyl substituents in the *meso*-linked moiety were generated in good yields. Full metalation of the dimers **6a**, **6d**, **6e**, or *rac*-**6h** to give the respective zinc(II), nickel(II), or copper(II) complexes **6a-Zn<sub>2</sub>**, **6a-Ni<sub>2</sub>**, **6a-Cu<sub>2</sub>**, **6d-Zn<sub>2</sub>**, **6e-Ni<sub>2</sub>**, and *rac*-**6h-Zn<sub>2</sub>** was easily achieved by known methods<sup>41</sup> in yields higher than 92%. In contrast to the synthesis of  $\beta$ , $\beta'$ -bisporphyrins, where the reaction course depends on the metalation states of the coupling partners,<sup>22</sup> the metal ion did not show a significant influence on the yields obtained in the case of the  $\beta$ ,*meso*-linked dimers. Hence, the coupling of precursors differing in their metalation states should permit free combination of two different metal centers within the bisporphyrin backbone, thus offering the possibility to selectively manipulate the properties of the desired dimers by the rational choice of the two central metals. In addition, variation of the *meso*-substituents of the  $\beta$ -borylated starting material can be expected to further expand the scope of the established method to most different substitution patterns of the accessible dimeric porphyrins: As

(36) (a) Moss, G. P. *Pure Appl. Chem.* **1987**, *59*, 799–832. (b) Moss, G. P. *Eur. J. Biochem.* **1988**, *178*, 277–573. (c) [www.chem.qmul.ac.uk/iupac/tetrapyrrole/](http://www.chem.qmul.ac.uk/iupac/tetrapyrrole/).

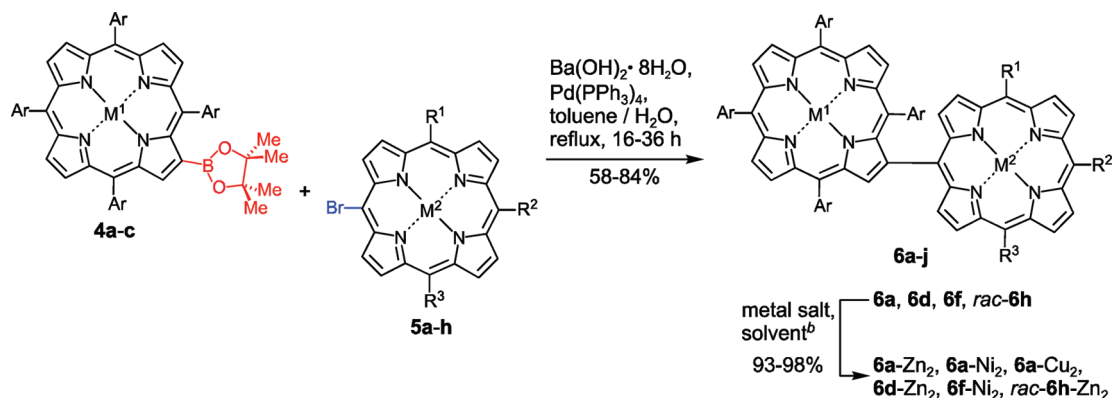
(37) For definitions and nomenclature of *meso*-substituted porphyrins, see: Lindsey, J. S. In *The Porphyrin Handbook*; Kadish, K. M., Smith, K. M., Guillard, R., Eds.; Academic Press: San Diego, 2000; Vol. 1, pp 45–118.

(38) (a) Miyaura, N.; Suzuki, A. *Chem. Rev.* **1995**, *95*, 2457–2483. (b) Suzuki, A. *Proc. Jpn. Acad.* **2004**, *80*, 359–371.

(39) The MacDonald [2 + 2]-type co-condensations were carried under standard Lindsey conditions: (a) Arsenault, G. P.; Bullock, E.; MacDonald, S. F. *J. Am. Chem. Soc.* **1960**, *82*, 4384–4389. (b) Lindsey, J. S.; Hsu, H. C.; Schreimann, I. C. *Tetrahedron Lett.* **1986**, *27*, 4969–4970.

(40) For a representative bromination protocol, see: Arnold, D. P.; Bott, R. C.; Eldridge, H.; Elms, F. M.; Smith, G.; Zojaji, M. *Aust. J. Chem.* **1997**, *50*, 495–503.

(41) For the insertion of zinc(II), see: (a) Adler, A. D.; Longo, F. R. *J. Inorg. Nucl. Chem.* **1970**, *32*, 2443–2445. For the insertion of nickel(II), see: (b) Richeter, S.; Hadj-Aissa, A.; Taffin, C.; van der Leebe, A.; Leclercq, D. *Chem. Commun.* **2007**, 2148–2150. For the insertion of copper(II), see: (c) Hosseini, A.; Taylor, S.; Accorsi, G.; Armaroli, N.; Reed, C. A.; Boyd, P. D. W. *J. Am. Chem. Soc.* **2006**, *128*, 15903–15913.

TABLE 2. Synthesis of  $\beta$ ,*Meso*-Linked Bisporphyrins by Suzuki Coupling of *Meso*-Brominated Porphyrins with  $\beta$ -Borylated TAPs<sup>a</sup>

Ar	M <sup>1</sup>	reactant	R <sup>1</sup>	R <sup>2</sup>	R <sup>3</sup>	M <sup>2</sup>	reactant	product (yield (%)) <sup>c</sup>	type
Ph	2H	<b>4a</b>	Ph	Ph	Ph	2H	<b>5a</b>	<b>6a</b> (65)	A <sub>3</sub> - $\beta$ TAP
Ph	2H	<b>4a</b>	Ph	Ph	Ph	Zn	<b>5b</b>	<b>6b</b> (58)	A <sub>3</sub> - $\beta$ TAP
Ph	2H	<b>4a</b>	Ph	Ph	Ph	Ni	<b>5c</b>	<b>6c</b> (66)	A <sub>3</sub> - $\beta$ TAP
Ph	2H	<b>4a</b>	<i>n</i> -Hex	<i>n</i> -Hex	<i>n</i> -Hex	2H	<b>5d</b>	<b>6d</b> (50)	A <sub>3</sub> - $\beta$ TAP
Ph	2H	<b>4a</b>	Ph	H	Ph	2H	<b>5e</b>	<b>6e</b> (65)	5,15-A <sub>2</sub> - $\beta$ TAP
4-ClPh	2H	<b>4b</b>	Ph	H	Ph	2H	<b>5e</b>	<b>6f</b> (48 <sup>d</sup> )	5,15-A <sub>2</sub> - $\beta$ TAP
Ph	2H	<b>4a</b>	3,5-di- <i>t</i> -BuPh <sup>e</sup>	Ph	3,5-di- <i>t</i> -BuPh <sup>e</sup>	2H	<b>5f</b>	<b>6g</b> (81)	5,15-A <sub>2</sub> B- $\beta$ TAP
Ph	2H	<b>4a</b>	4-MeOPh	H	<i>n</i> -Hex	2H	<b>5g</b>	<i>rac</i> - <b>6h</b> (84)	5,15-AB- $\beta$ TAP
Ph	Zn	<b>4c</b>	4-MeOPh	H	<i>n</i> -Hex	2H	<b>5g</b>	<i>rac</i> - <b>6i</b> (82)	5,15-AB- $\beta$ TAP
Ph	2H	<b>4a</b>	4-MeOPh	<i>n</i> -Hex	Ph	2H	<b>5h</b>	<i>rac</i> - <b>6j</b> (74)	ABC- $\beta$ TAP

<sup>a</sup>Reactions were carried out under Ar with porphyrin  $\beta$ -boronic acid ester **4** (1.0 equiv), *meso*-bromoporphyrin **5** (0.7–2.0 equiv), Ba(OH)<sub>2</sub>·8H<sub>2</sub>O (10 equiv), and Pd catalyst (20 mol %). <sup>b</sup>Zn(OAc)<sub>2</sub>·2H<sub>2</sub>O (10 equiv) or Cu(OAc)<sub>2</sub> (1.5 equiv) in CHCl<sub>3</sub>/MeOH, or Ni(acac)<sub>2</sub> (2.5 equiv) in toluene. <sup>c</sup>Isolated, nonoptimized yields. <sup>d</sup>**4b** was reisolated in 19% yield. <sup>e</sup>3,5-di-*t*-BuPh = 3,5-di-*tert*-butylphenyl.

an example, coupling of the  $\beta$ -boronic acid ester **4b** derived from 5,10,15,20-tetra(4-chlorophenyl)porphyrin<sup>42</sup> resulted in the formation of an 5,15-A<sub>2</sub>- $\beta$ TAP-type dimer **6f** having an electron-poor TAP subunit, albeit in a decreased yield of 48% (along with 19% recovered starting material **4b**), due to the low reactivity of the deactivated borylated precursor **4b**.

Even structurally more complex bisporphyrins were obtained in excellent yields using heterogeneously *meso*-substituted precursors such as 5-bromo-10,20-bis(di-*tert*-butylphenyl)-15-phenylporphyrin (**5f**), 5-bromo-10-*n*-hexyl-20-(4-methoxyphenyl)porphyrin (**5g**),<sup>43</sup> or 5-bromo-10-phenyl-15-*n*-hexyl-20-(4-methoxyphenyl)porphyrin (**5h**)<sup>43</sup> as demonstrated by the synthesis of the 5,15-A<sub>2</sub>B- $\beta$ TAP-, 5,15-AB- $\beta$ TAP-, and ABC- $\beta$ TAP-type bisporphyrins **6g**<sup>44</sup> and *rac*-**6h–j** (Table 2). Altogether, the synthetic strategy presented herein provides a modular principle for the generation of a broad structural diversity of  $\beta$ ,*meso*-linked bisporphyrins suitable for most different applications.

**Synthesis of Constitutionally Symmetric  $\beta$ ,*meso*-Linked Porphyrin Triads.** Besides the synthesis of  $\beta$ ,*meso*-linked porphyrin dimers, the established strategy also offers an easy entry into the design of trimeric porphyrins featuring two direct porphyrin–porphyrin axes: Starting from dibrominated 5,15-diphenylporphyrin **7a**, the  $\beta$ TAP-5,15-A<sub>2</sub>- $\beta$ TAP

trimer **8a** was synthesized in which two identical TAPs were  $\beta$ -linked to the central porphyrin macrocycle in a linear array (Table 3). Due to hindered rotation about the porphyrin–porphyrin axes, **8a** exists as a mixture of diastereomers, *cis*-**8a** and *trans*-**8a**, which were resolved by column chromatography on standard silica gel.<sup>45</sup> The product ratios of *cis*-**8a** and *trans*-**8a** (*cis/trans* = 1:2) obtained after isolation reflect the fact that the *cis*-geometry, i.e., with the C20' and C20'' aryl moieties being on the same side of the central macrocycle, is sterically much more demanding than the *trans*-orientation, with its “inner” phenyl rings (i.e., at C20' and C20''), which point toward the central porphyrin subunit, being located at opposite sides. A detailed discussion of the spatial arrangement of **8a** is given in the stereochemistry section.

Similar to the preparation of dimeric porphyrins, structurally even more differentiated trimers were synthesized, this time starting from 5,15-dibromo-10-*n*-hexyl-20-(4-methoxyphenyl)porphyrin (**7b**).<sup>43</sup> The  $\beta$ TAP-5,15-AB- $\beta$ TAP triad **8b**, which was thus accessible in excellent yields, was again obtained as a mixture of diastereomers, *cis*-**8b** and *trans*-**8b** (product ratio *cis/trans* = 1:1.5; Table 3). Full metalation<sup>41</sup> of *trans*-**8a** with zinc(II) was achieved in 94% yield.

Triporphyrins of this type had already been synthesized before, by co-condensation of  $\beta$ -formyl porphyrins and dipyrromethane, yet only in small quantities and poor combined yields of about 10% (product ratio *cis/trans* = 1:1).<sup>28</sup> The isolated yields using our optimized C–C coupling

(42) For the synthesis of **4b**, see ref 22.

(43) This compound has not been described in the literature so far. For its synthesis, see the Supporting Information.

(44) The fact that two signals are observed for the *tert*-butyl groups indicates that both the rotation about the porphyrin–porphyrin and around the porphyrin–(3,5-di-*tert*-butylphenyl) axes is restricted. A similar phenomenon had already been observed for *meso,meso'*-linked bisporphyrins.<sup>17</sup>

(45) For a *meso,meso'*-linked porphyrin trimer that was isolated as a mixture of atropo-diastereomers with relative *cis*- or *trans*-orientations, see ref 17.

**TABLE 3. One-Step Formation of Constitutionally Symmetric  $\beta$ ,*Meso*-Linked Porphyrin Triads by a 2-Fold Suzuki Coupling of 5,15-Dibrominated Porphyrins with  $\beta$ -Borylated TAPs<sup>a</sup>**

Ar	M <sup>1</sup>	reactant	R <sup>1</sup>	R <sup>2</sup>	M <sup>2</sup>	reactant	product (yield (%)) <sup>b</sup>	type
Ph	2H	<b>4a</b>	Ph	Ph	2H	<b>7a</b>	<i>cis</i> - <b>8a</b> (27) <i>trans</i> - <b>8a</b> (52)	$\beta$ TAP-5,15-A <sub>2</sub> - $\beta$ TAP
Ph	2H	<b>4a</b>	4-MeOPh	<i>n</i> -Hex	2H	<b>7b</b>	<i>cis</i> - <b>8b</b> (29) <i>trans</i> - <b>8b</b> (42)	$\beta$ TAP-5,15-AB- $\beta$ TAP

<sup>a</sup>Reactions were carried out under Ar with porphyrin  $\beta$ -boronic acid ester **4** (2.5 equiv), *meso*-bromoporphyrin **5** (1.0 equiv), Ba(OH)<sub>2</sub>·8H<sub>2</sub>O (10–20 equiv), and Pd catalyst (20 mol %). <sup>b</sup>Isolated, nonoptimized yields.

procedure<sup>22</sup> (combined yields 71–79%), by contrast, are excellent, proving the efficiency of the method established here. Thus, for the first time, the desired trimers are now available in one simple coupling step, e.g., at a 200-mg scale.

Furthermore, coupling of metalated dibromoporphyrins with  $\beta$ -borylated TAPs bearing a different metal center should result in the formation of trimers combining two identical central metals in the peripheral subunits with another, different one in the central porphyrin core. Thus, the synthetic procedure elaborated here permits rapid generation of a large variety of  $\beta$ ,*meso*-linked porphyrin triads, differing in their substitution pattern, in the metalation states of the subunits, and, in addition, in the spatial arrangement (e.g., *cis/trans*-geometry) of the chromophores. Finally, conversion of 5,10-diaryl-15,20-dibromoporphyrins will offer the possibility to synthesize  $\beta$ ,*meso*-linked trimers with an angular array of the three porphyrin units as yet another structural modification of the linear arrangement reported in the present work.<sup>46,47</sup>

**Functionalization of Preformed  $\beta$ ,*meso*-Linked Bisporphyrins.** In contrast to the above-described one-step synthesis of constitutionally symmetric porphyrin triads, the construction of constitutionally unsymmetric triporphyrins required the stepwise formation of the trimeric porphyrin backbone, either by the chemoselective transformation of difunctionalized monomeric porphyrins (e.g., 5-bromo-15-iododiarylporphyrins)<sup>48</sup> or by the directed preparation of an initially *meso*-free dimer, with subsequent halogenation and renewed

C–C coupling with a suitable monomeric porphyrin. In order to enable a divergent modification of the precious dimeric porphyrins at a late stage of the synthesis, the second alternative seemed preferable. Therefore, adequately functionalized bisporphyrins had to be synthesized to permit subsequent C–C coupling reactions.

The porphyrin dimers thus prepared can contain a free *meso*-position (see, e.g., **6e**, **6f**, *rac*-**6h**, and *rac*-**6i**, Table 2) amenable to further synthetic manipulations. As an example, the bisporphyrins **6e**, **6f**, and *rac*-**6i** were brominated<sup>40</sup> in good to excellent yields (82–99%, Table 4) giving the functionalized dimeric porphyrins **9a**, **9b**, and *rac*-**9c**, respectively.

The brominated dimers also permit introduction of another, different *meso*-substituent by a C–C coupling reaction at a very late stage of the synthesis yielding 5,15-A<sub>2</sub>B- $\beta$ TAP-type porphyrin dyads. Furthermore, a Miyaura transmetalation reaction<sup>49</sup> might give rise to *meso*-borylated bisporphyrins that can serve as versatile building blocks for the construction of complex porphyrin multichromophores.<sup>50</sup>

Moreover, the introduction of another *meso*-substituent succeeded, through nucleophilic attack of organolithium reagents<sup>34</sup> such as phenyllithium (PhLi) followed by quenching with H<sub>2</sub>O and oxidation with DDQ in acceptable yields (*rac*-**9d**, 43%, Table 4). It is noteworthy that the reaction takes place with a good regioselectivity at the free *meso*-position, C5. Reaction of the more reactive nucleophile *n*-hexyllithium (*n*-HexLi) with **6e** or the fully nickelated bisporphyrin **6e**–Ni<sub>2</sub>, however, resulted in a complex, inseparable

(46) The synthesis of such systems is currently under investigation in our groups.

(47) For *meso,meso'*-linked triporphyrins displaying such a rectangular geometry as synthesized by a Suzuki coupling, see ref 19.

(48) For a stepwise chemoselective functionalization of 5-bromo-15-iododiarylporphyrins leading to unsymmetric monomeric TAP derivatives, see: Shanmugathan, S.; Johnson, C. K.; Edwards, C.; Matthews, K.; Dolphin, D.; Boyle, R. W. *J. Porphyrins Phthalocyanines* **2000**, *4*, 228–232.

(49) Hyslop, A. G.; Kellett, M. A.; Iovine, P. M.; Therien, M. J. *J. Am. Chem. Soc.* **1998**, *120*, 12676–12677.

(50) For the synthesis of borylated *meso,meso'*-bisporphyrins and *meso,meso'*-linked porphyrin tetramers, see: Hori, T.; Aratani, N.; Takagi, A.; Matsumoto, T.; Kawai, T.; Yoon, M.-C.; Yoon, Z. S.; Cho, S.; Kim, D.; Osuka, A. *Chem.—Eur. J.* **2006**, *12*, 1319–1327.

TABLE 4. Further Functionalization of Bisporphyrins Having a Free *Meso*-Position

R <sup>1</sup>	R <sup>2</sup>	Ar	M <sup>1</sup>	M <sup>2</sup>	reactant	reaction conditions	X	product (yield (%)) <sup>a</sup>
Ph	Ph	Ph	2H	2H	<b>6e</b>	NBS/pyridine, 0 °C, 15 min	Br	<b>9a</b> (98)
Ph	Ph	4-ClPh	2H	2H	<b>6f</b>	NBS/pyridine, 0 °C, 30 min	Br	<b>9b</b> (82)
4-MeOPh	<i>n</i> -Hex	Ph	2H	Zn	<i>rac</i> - <b>6i</b>	NBS/pyridine, 0 °C, 15 min	Br	<i>rac</i> - <b>9c</b> (93)
4-MeOPh	<i>n</i> -Hex	Ph	2H	2H	<i>rac</i> - <b>6h</b>	(1) PhLi, 0 → 40 °C (2) H <sub>2</sub> O, 0 °C → rt (3) DDQ, rt	Ph	<i>rac</i> - <b>9d</b> (43)
Ph	Ph	Ph	2H	2H	<b>6e</b>	(1) HexLi, -5 → 40 °C (2) H <sub>2</sub> O, 0 °C → rt (3) DDQ, rt	<i>n</i> -Hex	complex mixture
Ph	Ph	Ph	Ni	Ni	<b>6e</b> -Ni <sub>2</sub>	(1) HexLi, -78 °C (2) H <sub>2</sub> O, -78 °C (3) DDQ, -78 °C	<i>n</i> -Hex	complex mixture

<sup>a</sup>Isolated, nonoptimized yields.

mixture of polyalkylated species and decomposition products even at -78 °C.

Besides synthetic manipulation at a free *meso*-position,<sup>51</sup> additional functionality can also be introduced by reactions at the periphery of the bisporphyrins. Some examples of such transformations are described in the stereochemistry part below.

In summary, the presented strategy will permit access to a plethora of 5,15-A<sub>2</sub>B-βTAP-type porphyrin dyads differing in their substituent B starting from preformed bisporphyrins by regioselective nucleophilic attack of organolithium reagents on a free *meso*-position.<sup>34</sup> In addition, the established protocols provide useful precursors, such as the brominated porphyrin dimers **9a**, **9b**, *rac*-**9c**, which, besides their use for the diverging introduction of *meso*-substituents at a late stage of the synthesis, can facilitate the construction of even larger, superstructured—chiral or achiral—oligoporphyrins, by simple C–C coupling reactions.

**Synthesis of Constitutionally Unsymmetric β,*Meso*-Linked Porphyrin Triads.** As expected, the functionalized dimers thus generated were not only useful for the divergent synthesis of a broad variety of unsymmetrically substituted bisporphyrins but proved to be versatile precursors for the construction of highly complex porphyrin trimers (βTAP-5,15-AB-βTAP' type) incorporating up to three different metal centers, two different substituents in the positions 10 and 20, and two differently substituted TAP moieties in the positions 5 or 15, as shown by the synthesis of **10** (Scheme 1). Directly linked trimeric porphyrins of comparable structural complexity have not been described in the literature so far.

As compared to the synthesis of the porphyrin triads *cis/trans*-**8a** and *cis/trans*-**8b** (*cis/trans* = 1:2 and 1:1.5, respectively), the higher portion of *trans*-configured atro-

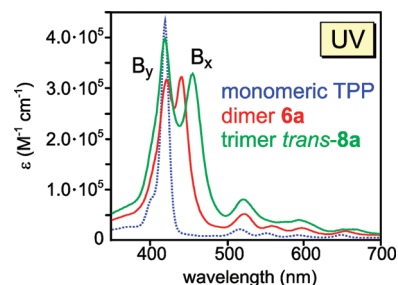


FIGURE 2. Typical UV/vis profiles of β,*meso*-linked dimeric and trimeric porphyrins in dichloromethane, exemplarily shown for the dimer **6a** and the trimer *trans*-**8a**, in comparison with the UV/vis spectrum of TPP.

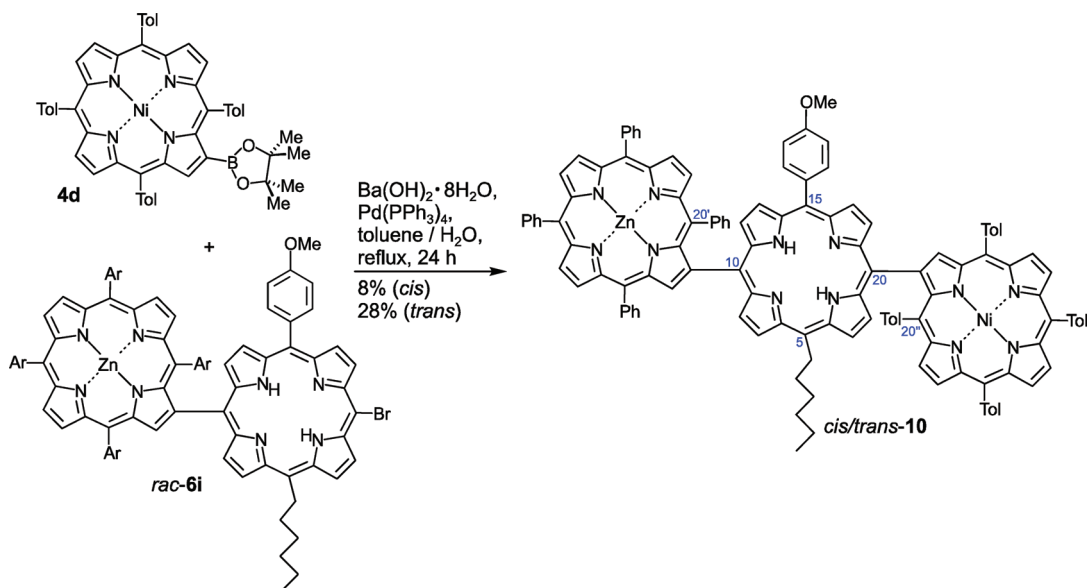
po-dia stereoisomer (*cis/trans* = 1:3.5) and the generally decreased yields (71–79% overall yield for **8a/b** as compared to 36% for **10**) obtained in the synthesis of **10** reflect the increased steric hindrance of *cis*-**10** due to the *para*-methyl group of the C20' tolyl moiety (see also Figure 4). The additional formation of traces of trimeric byproducts resulting from metal scrambling further contributed to the lowered yields.

**Spectral Properties of β,*Meso*-Linked Oligoporphyrins.** As expected, the UV/vis spectra of the free-base multichromophores, **6a–j**, *cis/trans*-**8a**, *cis/trans*-**8b**, **9a–f**, and **10** showed the B band (Soret band) at about 425 nm and the four Q bands between 480 and 680 nm. In contrast to the UV/vis spectrum of monomeric TPP, the Soret bands of dimeric and trimeric porphyrins were broadened and split due to the exciton coupling between the porphyrin subunits (Figure 2), in analogy to other β,*meso*-coupled bisporphyrins and in perfect accordance with the exciton coupling theory.<sup>52</sup>

(51) Further synthetic manipulations at a free *meso*-position of β,*meso*-linked bisporphyrins by, e.g., nitration (with subsequent reduction to *meso*-amino substituted bisporphyrins) or Vilsmeier formylation are currently under investigation.

(52) (a) Harada, N.; Nakanishi, K. *Circular Dichroic Spectroscopy: Exciton Coupling in Organic Stereochemistry*; University Science Books: Mill Valley, CA, 1983. (b) Rodger, A.; Nordén, B. *Circular Dichroism and Linear Dichroism*; University Press: Oxford, 1997.

## SCHEME 1. Synthesis of the Constitutionally Unsymmetric Triporphyrin 10



Consequently, a significant Davydov splitting of the B bands was observed, with an energy gap  $\Delta E$  (energetic difference between the  $B_y$  and the  $B_x$  bands) of about 1200 and 1600  $\text{cm}^{-1}$  for the  $\beta$ ,*meso*-linked dimers and trimers, respectively. In contrast to the dimeric porphyrins, the  $\beta$ ,*meso*-triporphyrins furthermore displayed a slight splitting of the energetically lower Q bands ( $\Delta E$  about 650  $\text{cm}^{-1}$ ).

The  $\Delta E$  values observed for the  $\beta$ ,*meso*-linked dimers correlate with typical splittings reported for similar literature-known systems with a  $\beta$ ,*meso*-linkage<sup>30</sup> and, thus, range between those of  $\beta$ , $\beta'$ -<sup>22,24</sup> and *meso*,*meso'*-coupled<sup>30</sup> bisporphyrins, which show characteristic B-band splittings of about 800 and 2100  $\text{cm}^{-1}$ , respectively. For  $\beta$ ,*meso*-linked triporphyrins, no exciton coupling energies have so far been reported. The free-base  $\beta$ ,*meso*-linked triads gave  $\Delta E$  values around 1800  $\text{cm}^{-1}$ , while slightly increased splitting energies were observed for the fully metalated derivatives ( $\Delta E$  value of *trans*-**8a**– $\text{Zn}_3$ ; 1950  $\text{cm}^{-1}$ ). As compared to zincated *meso*,*meso'*-linked porphyrin trimers ( $\Delta E = 3200 \text{ cm}^{-1}$ )<sup>19</sup> the peak splitting thus seems to be less significant following the trend of decreasing splitting energies from the *meso*,*meso'*- via the  $\beta$ ,*meso*- to the  $\beta$ , $\beta'$ -linkage as observed for differently linked bisporphyrins. The *cis*-configured diastereomers *cis*-**8a**, *cis*-**8b**, and *cis*-**10** displayed UV profiles nearly identical to those of the *trans*-analogues *trans*-**8a**, *trans*-**8b**, and *trans*-**10**.

In comparison to the Soret band of TPP, the  $B_y$  bands of the novel porphyrin dimers and trimers appeared almost unchanged regarding their wavelengths, whereas the  $B_x$  and Q bands were red-shifted. In general, the Q-band absorptions showed increased intensities, while the B band intensities were slightly decreased as compared to the respective bands in TPP.<sup>53</sup>

As expected, full metalation of the dimeric and trimeric porphyrins gave rise to a higher molecular symmetry and, thus, to a degeneration of the Q transitions resulting in a

decreased number of Q bands. The structurally complex porphyrin trimer **10** shows a UV profile that can be perceived as the superposition of a metal free and a fully metalated triporphyrin (see the Supporting Information).

**Characteristic NMR Properties.** Depending on the proximity of the four different phenyl groups of the  $\beta$ -coupled subunits relative to the central porphyrin–porphyrin axis, their protons were found to vary largely in <sup>1</sup>H NMR with respect to the chemical shifts (Figure 3a,b). Especially the central phenyl residues located above the *meso*-linked porphyrin macrocycle showed signals strongly shifted toward higher field. Due to a  $\pi$ -stacking interaction between these phenyl substituents and the adjacent, nearly coplanar-arranged porphyrin, they exhibited the most pronounced ring current affected chemical shifts.<sup>54</sup>

Thus, for all dimeric porphyrins and for the *trans*-configured trimers, the *para*-protons of the phenyl moiety at C20' (and C20'' for the trimers, see Scheme 1) appeared around 4.00 ppm (instead of 7.77 ppm in TPP), the *meta*-protons were shifted to about 4.70 ppm (instead of resonating at 8.22 ppm as in TPP), and the *ortho*-protons were found in the region from 6.75 to 6.95 ppm (instead of 7.77 ppm in TPP).<sup>55</sup> However, in the trimers possessing a *cis*-relationship between the central phenyl moieties at C20' and C20'', the protons seemed to be less affected by the ring current as compared to the corresponding *trans*-diastereomers: The respective *para*-protons resonated around 4.90 ppm, the *meta*-protons appeared at 5.40 ppm, and the *ortho*-protons were shifted to the region of 7.20 to 7.40 ppm, thus hinting at a conformation of the *cis*-configured compounds in which the central phenyl residues have “slipped” toward the magnetically less shielding periphery<sup>56,57</sup> of the coplanar porphyrin moiety (see also Figures 6 and 8). This may be due to

(54) This characteristic upfield shift for the central phenyl residues had previously been observed for similar dimeric porphyrin systems.<sup>22,28</sup>

(55) For a <sup>1</sup>H NMR spectrum of TPP, see ref 22b.

(56) (a) Cross, K. J.; Crossley, M. J. *Aust. J. Chem.* **1992**, *45*, 991–1004. (b) Abraham, R. J.; Smith, K. M. *J. Am. Chem. Soc.* **1983**, *105*, 5734–5741.

(57) Iwamoto, H.; Horib, K.; Fukazawaa, Y. *Tetrahedron Lett.* **2005**, *46*, 731–734.

(53) Especially for the highly unsymmetric derivatives a more detailed assignment of electronic transitions and explicit discussion of the excitonic effects in all multiporphyrins synthesized is hampered by a strong overlap of multiple B bands, which is caused by the low symmetry of the compounds.

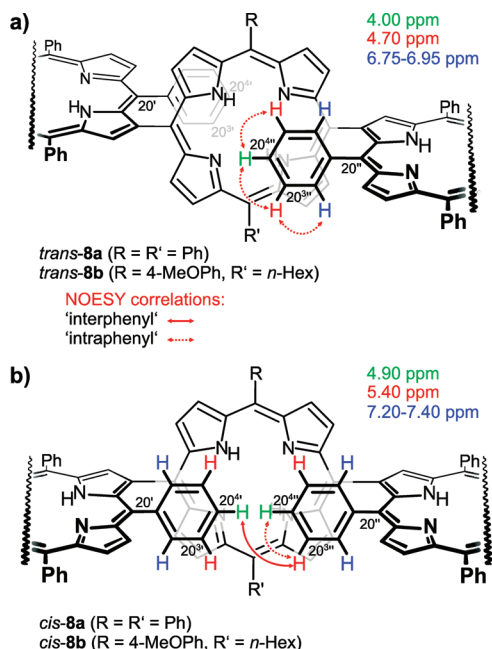


FIGURE 3. Characteristic NMR shifts and selected NOESY correlations of (a) *trans*-8a/b and (b) *cis*-8a/b.

additional steric constraints of the two central aryl substituents being located on the same side of the central porphyrin macrocycle.

A confirmation of this first, preliminary assignment of the *cis*- and the *trans*-configured trimers based on the chemical shifts of the protons of the C20' and C20'' phenyl moieties by ROESY correlations was, however, not trivial, because, for *cis*-8a and *cis*-8b, the corresponding *ortho*-, *meta*-, or *para*-protons of the two phenyl substituents (C20' and C20'') are chemically equivalent due to their enantiotopic or homotopic relationship, thus precluding the observation of any ROESY interactions, e.g., between the two *para*-protons (C20<sup>4'</sup> and C20<sup>4''</sup>). On the other hand, a possible correlation between the *para*- and the *meta*-protons should result in a ROESY cross peak, but the "interphenyl" correlation (e.g., between the C20<sup>4'</sup> *para*-H and the C20<sup>3''</sup> *meta*-H) cannot be distinguished from an "intraphenyl" interaction (e.g., between the C20<sup>4'</sup> *para*-H and the C20<sup>3'</sup> *meta*-H), since, again, the two *meta*-protons (C20<sup>3'</sup> and C20<sup>3''</sup>) are chemically equivalent. ROESY correlations should thus, in principle, be observed for both, the *cis*- and the *trans*-configured trimers, *cis*-8a,b and *trans*-8a,b (Figure 3a,b).

A robust assignment according to 2D NMR correlations was, however, easily possible for the highly unsymmetric trimer **10** equipped with two different aryl moieties in the core region: For the isomer of **10** with the less ring-current affected chemical shifts, the *para*-methyl substituent of the central C20'-tolyl moiety resonating at 0.35 ppm showed a clear, diagnostically highly significant, ROESY correlation with the *para*-proton (4.88 ppm) of the C20'-phenyl substituent (Figure 4b). Thus, this isomer was attributed the *cis*-configuration, while the other isomer, which gave no ROESY correlation between the *para*-methyl group (−1.31 ppm) of the C20'' residue and any of the five protons of the C20'-phenyl moiety, was evidenced to be *trans*-configured (Figure 4a).

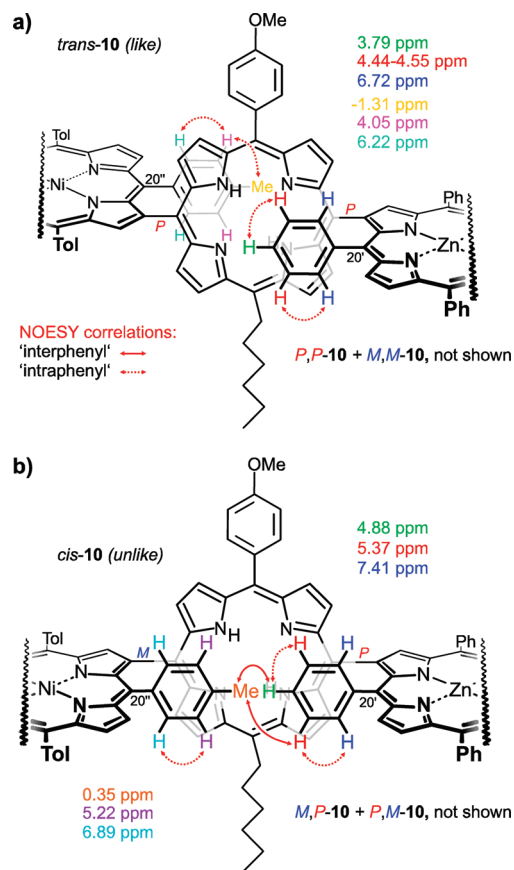


FIGURE 4. Characteristic NMR shifts and selected NOESY correlations of (a) *trans*-10 and (b) *cis*-10.

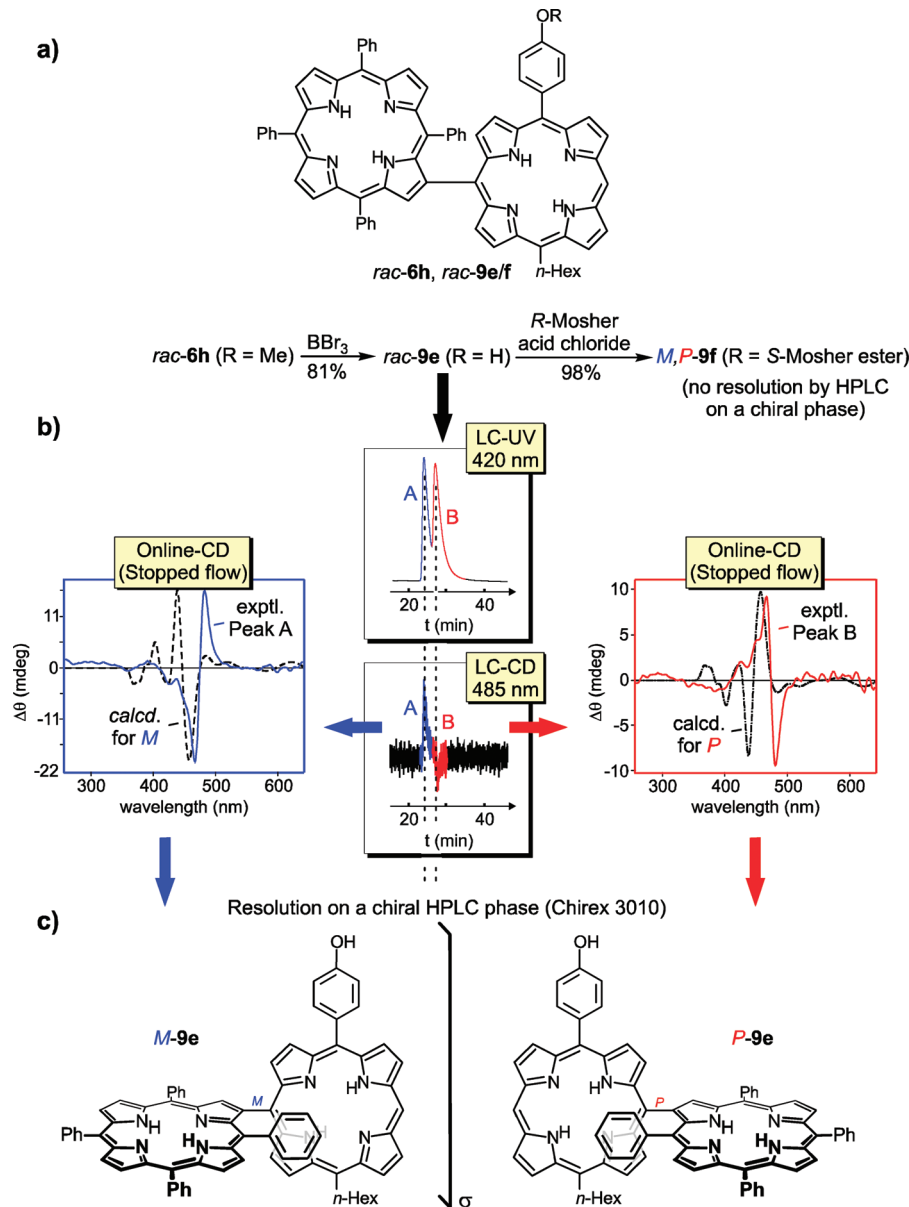
As a consequence, due to their close structural similarity, all trimers with the more downfield-shifted resonances of the central aryl moieties were assigned to be *cis*-configured, while the trimers exhibiting the less downfield shifted signals have the *trans*-configuration. These assignments are in line with the fact that the isomers that have thus been evidenced to be *trans*-configured are the main products of the coupling reactions, in agreement with their sterically less demanding array.

**Stereochemical Characterization of Chiral  $\beta$ ,Meso-Linked Porphyrin Dyads and Triads.** The new oligoporphyrins are interesting not only because of their physicochemical properties<sup>3,28</sup> but also because some of them show, in addition, rewarding stereochemical features. While the A<sub>3</sub>-, 5,15-A<sub>2</sub>-, and 5,15-A<sub>2</sub>B- $\beta$ TAP-type bisporphyrins **6a–g**, **9a**, and **9b** possess intramolecular mirror planes, which make them C<sub>s</sub>-symmetric, the constitutionally unsymmetric dimers *rac*-**6h–j**, *rac*-**6h–Zn<sub>2</sub>**, and *rac*-**9c–f** (5,15-AB- $\beta$ TAP type or ABC- $\beta$ TAP type) are C<sub>1</sub>-symmetric and, thus, axially chiral due to their heterogeneous substitution pattern (exemplarily shown for **6h**, **9e**, and **9f**, Scheme 2).<sup>58</sup>

The presumably chiral, C<sub>1</sub>-symmetric, and conformationally stable dimeric porphyrins **6h**, **6i**, **6h–Zn<sub>2</sub>**, and **9c–f** should exist as racemic mixtures of the two respective atropo-enantiomers. However, despite many attempts on a

(58) For an example of a *meso,meso'*-linked bisporphyrin with an achiral basic structure, which is, however, chiral due to its unsymmetric substitution pattern, see ref 17.

**SCHEME 2.** First Stereochemical Analysis of Axially Chiral  $\beta$ ,*Meso*-Bisporphyrins: (a) Chemical Derivatization of **6h** To Deliver **9e** and **9f**; (b) Comparison of the HPLC–CD Spectra (Measured in the Stopped-Flow Mode on a Chiral Phase) with the CD Curves Calculated Quantum Chemically (TDPBEO/6-31G\*); (c) Assigned Stereostructures of the *M*- and the *P*-Configured Atropo-Enantiomers, Exemplarily for the  $\beta$ ,*Meso*-Linked Bisporphyrin **9e**



variety of chiral HPLC phases under different chromatographic conditions, even at 0 °C, none of the bisporphyrins **6h**, **6i**, **9c**, or **9d** could be resolved into its expected enantiomers. Only for **6h**–Zn<sub>2</sub> was a slight “peak doubling” observed, but the separation was not sufficient to permit online-CD measurements. For this reason, a derivative of *rac*-**6h** with a more polar functional group was prepared, viz. the hydroxy-substituted dimer *rac*-**9e** (see Scheme 2): *O*-demethylation of the dimer *rac*-**6h**–Zn<sub>2</sub> with BBr<sub>3</sub><sup>59</sup> gave the hydroxy derivative *rac*-**9e** in 72% yield, accompanied by complete demetalation. Starting from the free-base bisporphyrin *rac*-**6h**, *rac*-**9e** was obtained in 81% yield.

This porphyrin dimer *rac*-**9e** now indeed gave a satisfying separation on a Chirex 3010 column (Phenomenex) at room temperature using *n*-hexane–dichloromethane (v/v 80:20, isocratic, flow: 0.7 mL/min) as the solvent system (Scheme 2). The novel dimers *rac*-**6h**–**j**, *rac*-**6h**–Zn<sub>2</sub>, *rac*-**9c**, and *rac*-**9c**–**f** are the first examples of axially chiral  $\beta$ ,*meso*-linked bisporphyrins described so far.

That the two resulting LC–UV peaks indeed corresponded to the two respective atropo-enantiomers of **9e** was clearly demonstrated by their opposite CD effects, as measured by LC–CD coupling in the stopped-flow mode, providing a positive CD signal for the faster eluting peak A and a negative one for the slower eluting peak B at 485 nm. For the determination of the absolute configurations of the two atropo-enantiomers, full online-CD spectra were

(59) (a) McOmie, J. F. W.; Watts, M. L.; West, D. E. *Tetrahedron* **1968**, *24*, 2289–2292. (b) Milgrom, L. R. *J. Chem. Soc., Perkin Trans. 1* **1983**, 2535–2539.

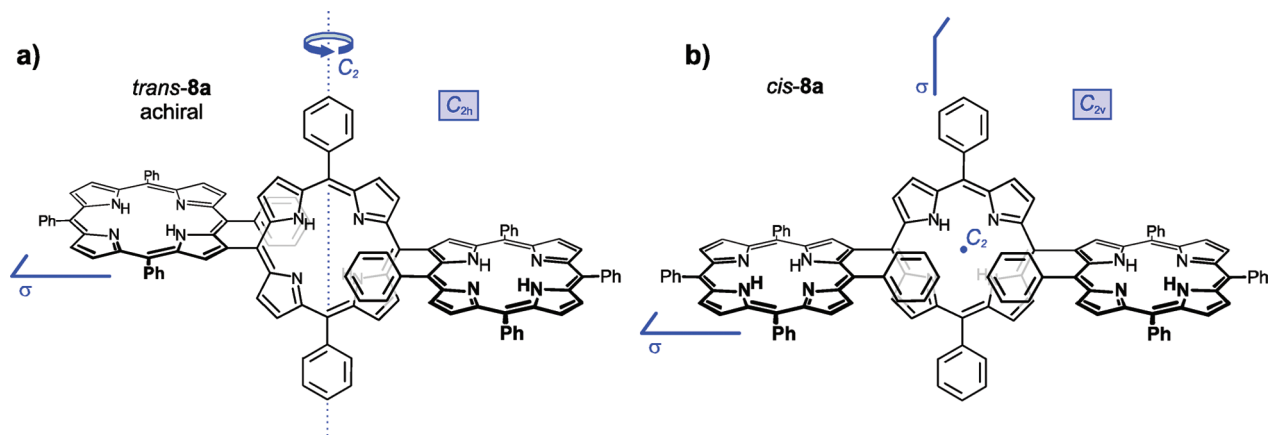


FIGURE 5. (a) Stereostructures of the  $C_{2h}$ -symmetric triporphyrin *trans*-**8a** and (b) of the  $C_{2v}$ -symmetric trimer *cis*-**8a**.

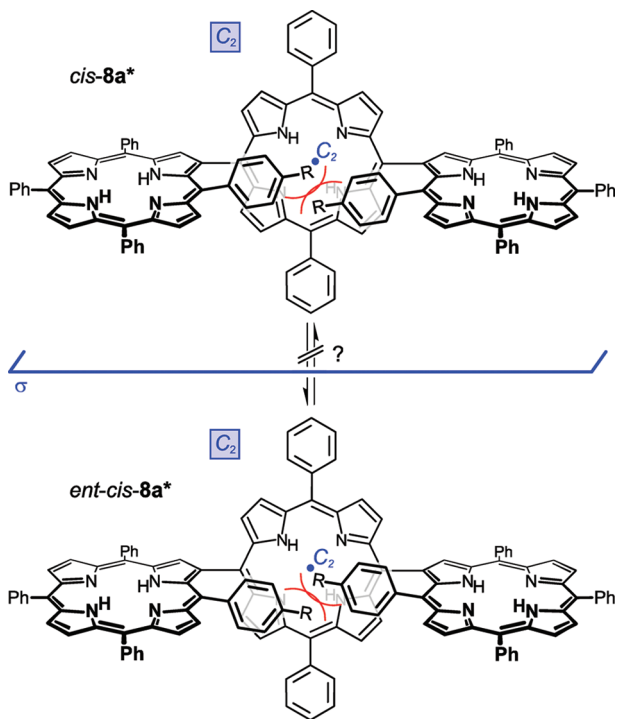


FIGURE 6. Possible  $C_2$ -symmetric chiral conformation of *cis*-**8a** that might be stereochemically stable depending on the size of the “inner” aryl groups.

recorded, giving mirror-imaged CD curves with a positive first Cotton effect around 485 nm for the faster and a negative one for the slower enantiomer.

These CD spectra revealed a remarkable feature: While in all other literature-known, axially chiral *meso,meso'*-<sup>17</sup> or  $\beta,\beta'$ -linked bisporphyrins,<sup>22</sup> the inflection points of the strongest CD effects correlate with the minimum between the  $B_y$  and the  $B_x$  band in the UV spectrum, the CD curves of **9e** display their major Cotton effects around 485 nm, i.e., red-shifted by about 55 nm.<sup>60</sup>

(60) A more detailed discussion of this finding is not possible without in-depth investigation of the electronic transitions of the bisporphyrin **9e** using, for example, MCD measurements in combination with quantum chemical calculations. This is currently under investigation.

For this reason and due to the fact that the dimer **9e** is highly unsymmetric ( $C_1$ -symmetry), attribution of its absolute configuration by application of the exciton chirality method<sup>52</sup> was not possible. Likewise excluded was an empirical comparison of its CD spectra with those of other porphyrin dimers, due to the unprecedented structure of **9e**. For this reason, quantum chemical CD calculations seemed to be the method of choice, despite the size of the molecule. Thus, the structure of the dimer **9e** was optimized with RI-PBE/SV(P)<sup>61,62</sup> in combination with a dispersion correction to take into account  $\pi,\pi$ -interactions between the phenyl substituent next to the axis and the adjacent porphyrin moiety.<sup>63</sup> TDPBEO/6-31G\*<sup>61,64</sup> calculations involving the first 45 excitations and a UV correction<sup>65</sup> of 50 nm finally yielded the calculated CD curves, which were then compared with the experimental ones. Accordingly, the faster peak A was evidenced to be *M*-configured while the slower eluting peak B was found to be *P*-configured. Thus, in the case of **9e**, application of the exciton chirality method<sup>52</sup> or comparison of the CD spectra with those of related porphyrin dimers would indeed have led to a wrong configurational assignment.<sup>66,67</sup>

Coming back to the enantiomeric resolution of *rac*-**9e**: While the chromatographic separation on a chiral phase succeeded after setting free the phenolic OH-group (see above), the respective Mosher derivatives<sup>68,69</sup> *S,M*-**9f** and

(61) Perdew, J. P.; Burke, K.; Ernzerhof, M. *Phys. Rev. Lett.* **1996**, *77*, 3865–3868.

(62) Schäfer, A.; Horn, H.; Ahlrichs, R. *J. Chem. Phys.* **1992**, *97*, 2571–7.

(63) Such  $\pi$ -stacking interactions had been substantiated for structurally related bisporphyrins by X-ray diffraction analysis.<sup>22</sup>

(64) (a) Perdew, J. P.; Burke, K.; Ernzerhof, M. *Phys. Rev. Lett.* **1997**, *78*, 1396. (b) Perdew, J. P.; Ernzerhof, M.; Burke, K. *J. Chem. Phys.* **1996**, *105*, 9982–9985. (c) Ernzerhof, M.; Scuseria, G. E. *J. Chem. Phys.* **1999**, *110*, 5029–5036. (d) Francl, M. M.; Pietro, W. J.; Hehre, W. J.; Binkley, J. S.; Gordon, M. S.; Defrees, D. J.; Pople, J. A. *J. Chem. Phys.* **1982**, *77*, 3654–3665. (e) Hariharan, P. C.; Pople, J. A. *Theor. Chim. Acta* **1973**, *28*, 213–22.

(65) Bringmann, G.; Bruhn, T.; Maksimenka, K.; Hemberger, Y. *Eur. J. Org. Chem.* **2009**, 2717–2727.

(66) For  $\beta,\beta'$ -bisporphyrins reported previously<sup>22</sup> the assignment of the absolute axial configuration by applying the exciton chirality approach was in agreement with the result of quantum chemical CD calculations; in general, however, the interpretation of CD spectra of directly linked dimeric porphyrins by the exciton chirality method is critical.<sup>67</sup>

(67) Muranaka, A.; Asano, Y.; Tsuda, A.; Osuka, A.; Kobayashi, N. *ChemPhysChem* **2006**, *7*, 1235–1240.

(68) Dale, J. A.; Dull, D. L.; Mosher, H. S. *J. Org. Chem.* **1969**, *34*, 2543–2549.

(69) The free hydroxy function of *rac*-**9e** permitted esterification with *R*-Mosher's acid chloride<sup>68</sup> on an analytical scale (1 mg) using triethylamine in dry  $\text{CH}_2\text{Cl}_2$  to yield *rac*-**9f** in quantitative yield: HRMS (ESI) calcd for  $\text{C}_{86}\text{H}_{66}\text{N}_8\text{O}_3\text{F}_3$  [ $\text{M} + \text{H}^+$ ] 1315.5205, found 1315.5205.

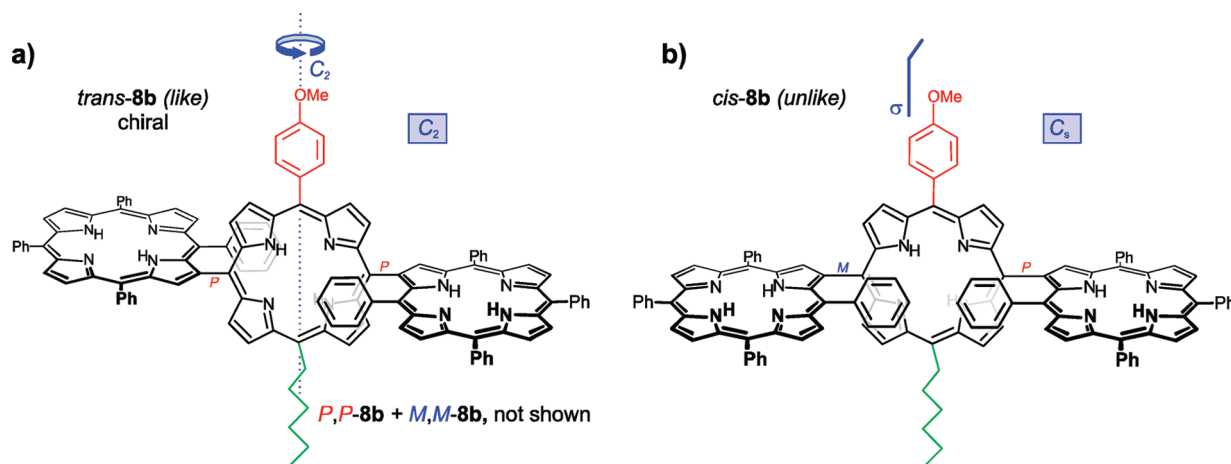


FIGURE 7. (a) Stereostructure of the chiral,  $C_2$ -symmetric trimer *trans-8b*. (b)  $C_3$ -symmetric meso-like conformation of *cis-8b*.

*S,P-9f*—despite being diastereomers!—could not be resolved, not even on a chiral phase.<sup>70</sup> Still, the free OH group of **9e** will be useful for other purposes, e.g., for the attachment of such porphyrin dimers to biomolecules<sup>71</sup> or dendrimeric backbones.<sup>72</sup>

In the case of the porphyrin trimers **8a**, **8b**, and **10**, the stereochemical analysis becomes more complex: As already mentioned, all trimers were formed as a diastereomeric mixture of two atropo-isomers, i.e. the “*trans*”-isomers with the two aryl substituents pointing toward the central porphyrin being located at opposite sides of the central macrocycle and the “*cis*”-isomers with the aryl moieties being on the same side (Figures 5 and 7).<sup>45</sup> For all porphyrin trimers synthesized the respective diastereomers were separable by column chromatography on usual silica gel. The ratios of the *cis*-configured isomers as compared to the *trans*-configured ones (*cis-8a/trans-8a* = 1:2, *cis-8b/trans-8b* = 1:1.5, and *cis-10/trans-10* = 1:3.5; Table 3 and Scheme 1) evidenced that the *cis*-orientation of the central phenyl rings is sterically more demanding than the *trans*-orientation.

(70) In addition, the Mosher derivative of **9e** did not give a double set of signals in <sup>1</sup>H NMR, as would have been expected for the two resulting diastereomers *S,M-9f* and *S,P-9f*. Most probably, the position of the stereocenter is too peripheral to influence, e.g., the protons of the central C2'-phenyl moiety.

(71) For a recent review on porphyrin bioconjugates, see: (a) Hudson, R.; Boyle, R. W. *J. Porphyrins Phthalocyanines* **2004**, *8*, 954–975 and references cited therein. For some recent, selected publications on porphyrin bioconjugates, see: (b) Sutton, J. M.; Fernandez, N.; Boyle, R. W. *J. Porphyrins Phthalocyanines* **2000**, *4*, 655–658. (c) Sutton, J. M.; Clarke, O. J.; Fernandez, N.; Boyle, R. W. *Bioconjugate Chem.* **2002**, *13*, 249–263. (d) Hudson, R.; Carcenac, M.; Smith, K.; Madden, L.; Clarke, O. J.; Pèlerin, A.; Greenman, J.; Boyle, R. W. *Br. J. Cancer* **2005**, *92*, 1442–1449. (e) Sibrian-Vazquez, M.; Jensen, T. J.; Fronczek, F. R.; Hammer, R. P.; Vicente, M. G. H. *Bioconjugate Chem.* **2005**, *16*, 852–863. (f) Borbas, K. E.; Mroz, P.; Hamblin, M. R.; Lindsey, J. S. *Bioconjugate Chem.* **2006**, *17*, 638–653. (g) Borbas, K. E.; Kee, H. L.; Holten, D.; Lindsey, J. S. *Org. Biomol. Chem.* **2008**, *6*, 187–194. (h) Jiang, M. Y.; Dolphin, D. *J. Am. Chem. Soc.* **2008**, *130*, 4236–4237. (i) Muresan, A. Z.; Lindsey, J. S. *Tetrahedron* **2008**, *64*, 11440–11448. (j) Sibrian-Vazquez, M.; Nesterova, I. V.; Jensen, T. J.; Vicente, M. G. H. *Bioconjugate Chem.* **2008**, *19*, 705–713.

(72) For selected reviews on dendrimeric porphyrins, see: (a) Venturi, M.; Serroni, S.; Juris, A.; Campagna, S.; Balzani, V. *Top. Curr. Chem.* **1998**, *197*, 193–228. (b) Jiang, D.-L.; Sadamoto, R.; Tomioka, N.; Aida, T. In *Hyper-Struct. Mol. I*; Sasabe, H., Ed.; Taylor & Francis, CRC Press: Boca Raton, FL, 1999; pp 63–73. (c) Aida, T.; Jiang, D.-L. In *The Porphyrin Handbook*; Kadishi, R. K., Smith, K. M., Guillard, R., Eds.; Academic Press: New York, 2000; Vol. 3, pp 369–384. (d) Balzani, V.; Ceroni, P.; Juris, A.; Venturi, M.; Campagna, S.; Puntoriero, F.; Serroni, S. *Coord. Chem. Rev.* **2001**, *219–221*, 545–572. (e) Jang, W.-D.; Nishiyama, N.; Kataoka, K. *Supramol. Chem.* **2007**, *19*, 309–314.

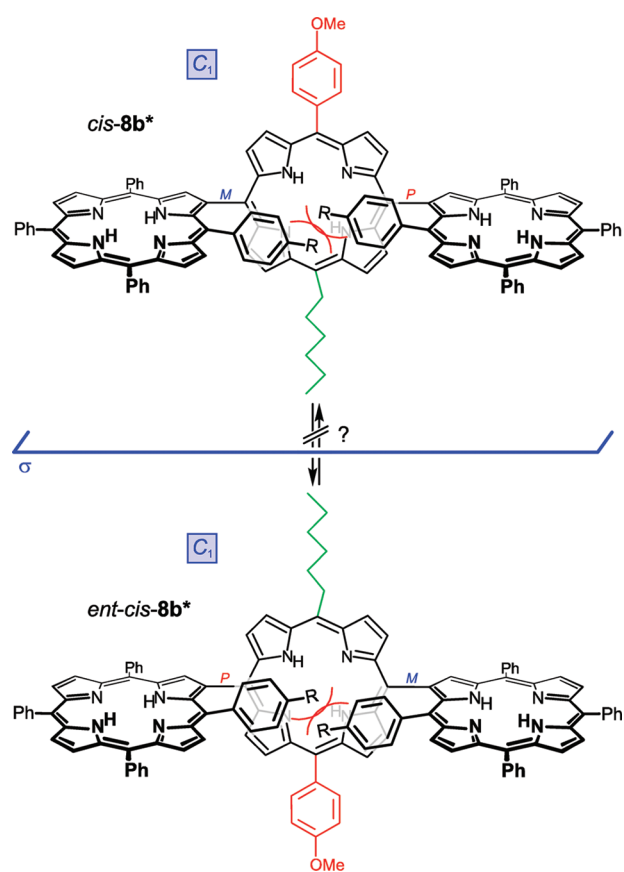
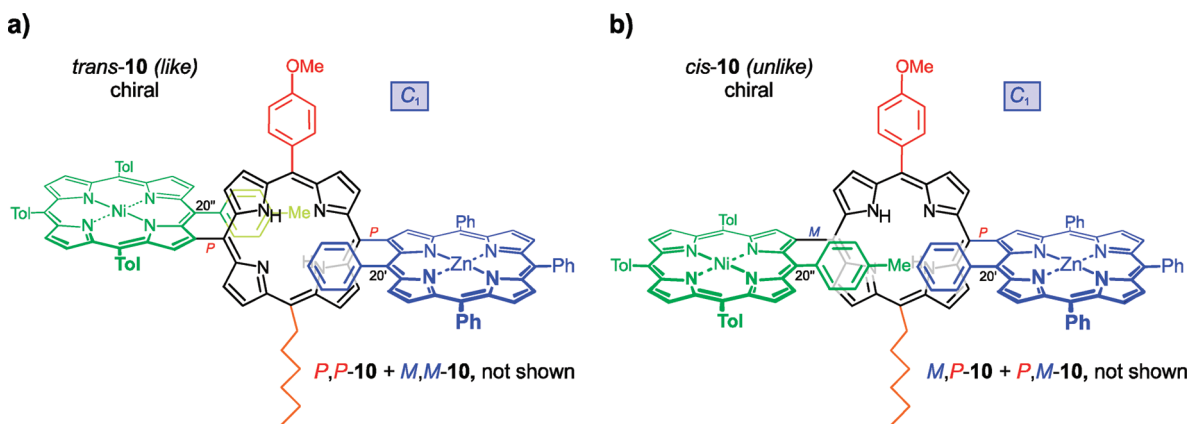


FIGURE 8. Chiral conformations of *cis-8b* with  $C_1$  symmetry, potentially stable depending on the temperature and the size of the substituent R (here investigated for R = H for *cis-8b*).

Due to their intramolecular mirror planes, the  $C_{2h}$ -symmetric  $\beta$ TAP- $A_2$ - $\beta$ TAP triporphyrin *trans-8a* (Figure 4a) and, in particular, the  $C_{2v}$ -symmetric trimer *cis-8a* (Figure 5b) should be achiral meso-compounds. This is indeed the case for *trans-8a* (Figure 5a). The *cis*-configured diastereomer *cis-8a*, however, although, at first sight, even possessing two planes of symmetry, actually still might be chiral depending on steric factors (Figure 6): Thus, if the size of the *para*-substituents R (R = H for *cis-8a*) was sufficiently



**FIGURE 9.** (a) Stereostructure of the chiral,  $C_1$ -symmetric trimer *trans*-**10**. (b) Chiral,  $C_1$ -symmetric porphyrin triad *cis*-**10**.

large to prevent the two central aryl moieties from passing each other, *cis*-**8a** should adopt a  $C_2$ -symmetric conformation and, as a consequence, exist in the form of two enantiomers, *cis*-**8a**\* and *ent-cis*-**8a**\* (Figure 6). In addition,  $\pi$ -stacking interactions between the phenyl substituents and the central porphyrin (as already substantiated by X-ray diffraction analysis for similar systems)<sup>22,28</sup> might contribute to the activation energy of the racemization process interconverting *cis*-**8a**\* and *ent-cis*-**8a**\*. At least in the case of sterically more demanding substituents R (like, e.g., for methyl or larger substituents), the rotational barrier should be high enough to guarantee conformational stability of such enantiomers. This stereochemical feature would be unique since, in contrast to all other axially chiral dimers reported so far, the chirality would not result from an intrinsically chiral  $\beta,\beta'$ -coupling<sup>22</sup> or (as required in the case of  $\beta,\text{meso}$ -<sup>28–30</sup> or *meso,meso'*-linked<sup>16–20</sup> dimers) from an unsymmetric substitution pattern but would arise from a stable chiral conformation of the otherwise symmetric porphyrin backbone itself, again independent from further unsymmetrically located substituents.

In contrast to *trans*-**8a**, the constitutionally unsymmetric porphyrin trimer *trans*-**8b** lacks an intramolecular plane of symmetry due to the heterogeneous 5,15-AB substitution pattern of the central porphyrin subunit (Figure 7a). Thus, the  $C_2$ -symmetric trimer *trans*-**8b** should exist as a racemic mixture of its two atropo-enantiomers, *P,P*-**8b** and *M,M*-**8b** (i.e., both with the same relative *like*-configuration). Unfortunately, despite intensive efforts, we did not succeed in resolving *trans*-**8b** into its atropo-enantiomers *P,P*-**8b** and *M,M*-**8b** by HPLC using different chiral stationary phases with various chromatographic conditions.

As already discussed in detail for *cis*-**8a**, the existence of stereochemically stable conformational enantiomers of *cis*-**8b** (i.e., with *unlike*-configuration, Figure 6b) should again depend on the sterical demand of the aryl residues that point toward the center of the triporphyrin and, thus, on the question whether, at a given temperature, *cis*-**8b** adopts an achiral, *meso*-like,  $C_s$ -symmetric conformation (averaged over time) or a stable chiral  $C_1$ -symmetric array (Figure 8). Although no chromatographic resolution of the supposed atropo-enantiomers succeeded as yet, clear hints at a chiral conformation of *cis*-**8b** at low temperatures were obtained, at

least on the NMR time scale. These VT-NMR investigations are discussed in detail below.

Due to its  $C_1$  symmetry, the structurally complex porphyrin triad **10** lacks any intramolecular mirror planes, for the *trans*-configuration (*trans*-**10**), and—in contrast to the above-discussed trimers *cis*-**8a** and *cis*-**8b**—also for the *cis*-configured isomer, *cis*-**10**. Consequently, besides *trans*-**10** (*like*-configuration, Figure 9a) even the *cis*-configured triporphyrin *cis*-**10** should be chiral, existing as a racemic mixture of two atropo-enantiomers, *M,P*-**10** and *P,M*-**10** (both with a relative *unlike*-configuration, Figure 9b). It is noteworthy that this chirality of *cis*-**10** is, in contrast to that of *cis*-**8a/b**, independent from the spatial arrangement of the central phenyl residues because it is  $C_1$ -symmetric and can, thus, never adopt a *meso*-like conformation.

The chirality of *cis*-**10** per se is combined with the additional chiral element resulting from the central aryl moieties (viz. the C20'-tolyl and the C20'-phenyl group), which might again adopt stable—now additionally diastereomeric—conformations, with these inner aryl residues “slipped” toward the periphery of the central porphyrin core. This constellation would, thus, give rise to the existence of now even four stereoisomers of *cis*-**10**, namely *M,P*-**10**, *P,M*-**10**, *M,P*-**10'**, and *P,M*-**10'** (Figure 10).

Resolution of the supposed stereoisomers did, however, not succeed by HPLC on a chiral phase. In analogy to the VT-NMR measurements performed for *cis*-**8b** (see the following text), further investigations of the highly unsymmetric triporphyrin *cis*-**10** by VT-NMR will shed light on the proposed existence of additional chiral stereogenic elements of such porphyrin trimers (besides the  $\beta,\text{meso}$ -axes) that are more or less stable on the NMR time scale. This work is in progress.

**Variable-Temperature  $^1\text{H}$  NMR Investigations of the Triporphyrin *cis*-**8b**.** To gain further insight into the dynamic behavior and, thus, into the chiral nature of the triporphyrins synthesized, low-temperature NMR measurements were performed, exemplarily for the *unlike*-configured trimer *cis*-**8b**.

As expected, the  $^1\text{H}$  NMR of *cis*-**8b** showed five signals for the 10 protons of the central phenyl residues at C20' and C20'' at room temperature (Figure 11).<sup>73</sup> Due to the

(73) At room temperature the signals of the *ortho*-protons (20<sup>3'</sup>/20<sup>5'</sup>- and 20<sup>3''</sup>/20<sup>5''</sup>-H) are partially covered by the CDCl<sub>3</sub> signal.

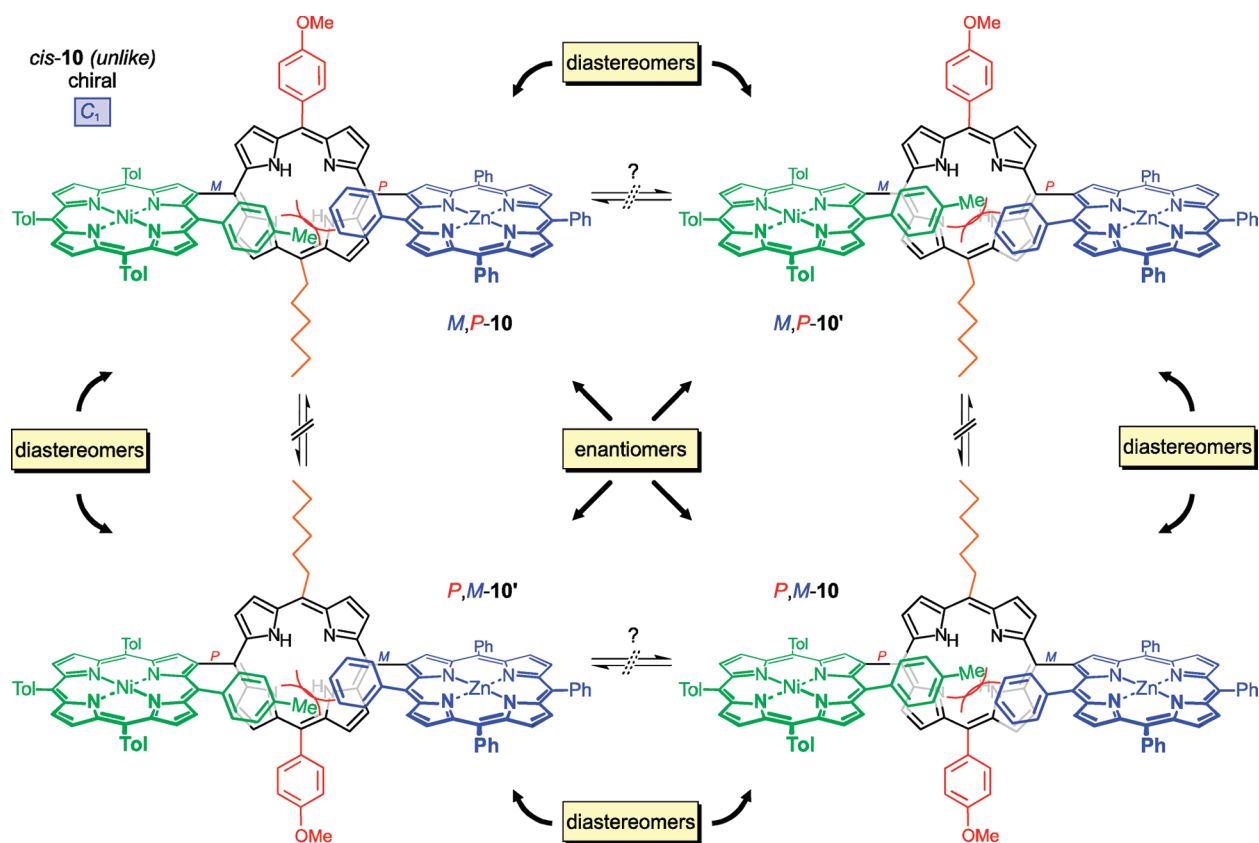


FIGURE 10. Four possible stereoisomers of *cis*-10 based on the assumption that—besides the two chiral axes—the conformational twisting of the central aryl moieties may constitute an additional stereogenic element.

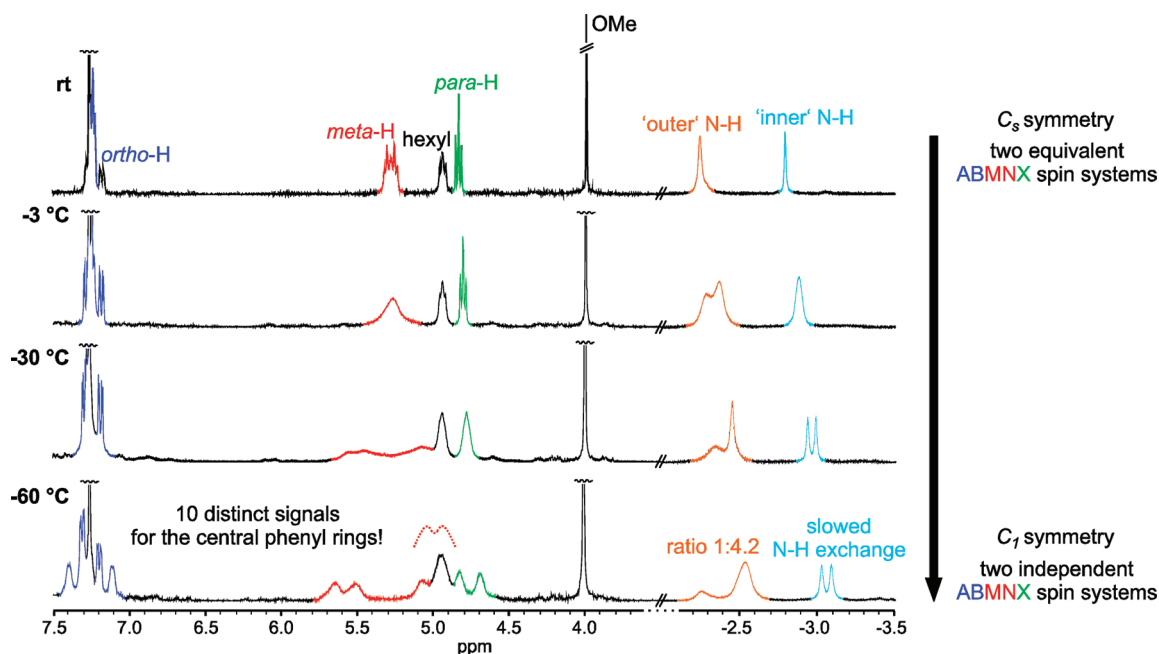


FIGURE 11. Variable-temperature NMR spectra of *cis*-8b showing 10 distinct signals for the protons of the "inner" phenyl substituents (one *meta*-H is covered by a hexyl resonance) at low temperatures.

$C_s$ -symmetric "average conformation" of *cis*-8b the corresponding *ortho*-, *meta*-, and *para*-protons (integrals 2:2:2:2) are pairwise homotopic, thus resulting in two equivalent

ABMN spin systems. Upon cooling, the resonances of the *meta*- and *para*-protons appeared broadened and finally split into a total of 10 distinct signals (including the resonances of

the *ortho*-protons) at  $-60$  °C. Thus, from the resulting two separated ABMN spin systems for the two central phenyl moieties, all protons of the “inner” phenyl substituents are nonequivalent under these conditions, and the molecule must have adopted a  $C_1$ -symmetric structure! This corroborates the assumption that the central aryl moieties (viz. the C20'-tolyl and the C20'-phenyl group) can attain stable conformations with these aryl residues “slipped” toward the periphery of the central porphyrin core, thus—besides the two chiral axes—providing an additional and different element of chirality which had not been recognized so far!

The NH protons of the “outer” porphyrin macrocycles were broadened, decreased in intensity, and split into two signals, surprisingly integrating in a ratio of 1:4.2. We attribute this finding to the existence of two “frozen” main NH-tautomers, differing in their relative stabilities.<sup>74</sup>

## Conclusion

In summary, a variable and straightforward procedure for the synthetic construction of achiral and chiral  $\beta$ ,*meso*-linked porphyrin arrays has been established. The key step of the synthesis was an optimized Suzuki coupling of  $\beta$ -borylated tetraarylporphyrins as previously synthesized for the first time by some of us.<sup>22</sup> Using an optimized C–C coupling protocol, several constitutionally symmetric and unsymmetric  $\beta$ ,*meso*-bisporphyrins—differing in their substitution pattern and in their metalation states—were efficiently prepared.

Furthermore, novel  $\beta$ ,*meso*-linked porphyrin trimers possessing two direct porphyrin–porphyrin axes have become available by the presented strategy in good yields and at a 200-mg scale. Thus, a broad structural diversity of  $\beta$ ,*meso*-linked porphyrin triads has been synthesized, again differing in their substitution pattern, in the metalation states of the subunits, and, in addition, in the spatial arrangement (*cis*- vs *trans*-geometry) of the chromophores.

The generated porphyrin dimers can contain a free *meso*-position amenable to further synthetic manipulations as shown, e.g., by the synthesis of the brominated dimers **9a**, **9b**, and *rac*-**9c**. These brominated bisporphyrins constitute valuable precursors for the synthesis of *meso*-borylated porphyrin dimers, which can serve as versatile building blocks for the construction of complex porphyrin multi-chromophores.<sup>50</sup> Moreover the introduction of another *meso*-substituent into a bisporphyrin with a free *meso*-position was achieved by addition of organolithium reagents followed by oxidation with DDQ,<sup>34</sup> as demonstrated by the successful synthesis of *rac*-**9d**. The reaction regioselectively takes place at the free *meso*-position of the bisporphyrin starting material. Thus, time-consuming multistep syntheses of highly functionalized bisporphyrins can be avoided by the late-stage divergent modification of preformed porphyrin dimers.

The broad applicability and the efficiency of the established procedures was finally demonstrated by the successful synthesis of the highly unsymmetric, axially chiral porphyrin

trimer **10** possessing two direct porphyrin–porphyrin axes, three different metal centers, two different substituents at C10 and C20, and two differently substituted TAP moieties in positions 5 and 10. Porphyrin trimers with a comparable structural complexity had not yet been described in the literature.

The novel compounds show remarkable stereochemical features. Thus, the bisporphyrins **6h**, **6i**, **6h**–Zn<sub>2</sub>, and **9c**–**f** were shown to exist as racemic mixtures as demonstrated by enantiomeric resolution of *rac*-**9e** by HPLC on a chiral phase in combination with online LC–CD measurements. Axially chiral  $\beta$ ,*meso*-linked bisporphyrins had not been reported before. The synthesized porphyrin trimers, by contrast, were even isolated as two configurationally stable atropo-diastereomers, the *trans*-isomers, with the two “inner” aryl substituents (i.e., those that point toward the central porphyrin) being located at opposite sides of the central macrocycle, and the *cis*-isomers, with the aryl moieties being on the same side. The novel  $C_2$ -symmetric porphyrin triads *trans*-**8b**, *trans*-**10**, and *cis*-**10** presented in this paper constitute the first examples of axially chiral  $\beta$ ,*meso*-linked triporphyrins. And even the *cis*-configured trimeric porphyrins *cis*-**8a** and *cis*-**8b**, although being *meso*-like—and thus achiral at first sight—are stereochemically intriguing, since they can, depending on the steric constraints, also adopt  $C_1$ -symmetric (and thus chiral) conformations, as proven by detailed VT-NMR investigations of the triporphyrins. To the best of our knowledge, chirality originating from a similar phenomenon has not been observed so far. This makes the synthesis of related, but sterically more congested, *cis*-configured porphyrin trimers possibly existing as two configurationally *stable* enantiomers already at room temperature, a rewarding task. This work is currently in progress.

The synthetic results show that the presented protocols permit a rapid generation of a plethora of structurally diverse, constitutionally unsymmetric oligoporphyrins with enhanced optical properties and unexpected stereochemical features. Moreover, the introduced synthetic strategy is applicable to the construction of amphiphilic porphyrin dimers and trimers for use in photodynamic therapy and for the synthesis of push–pull chromophores for optical applications, and it can provide useful precursors for the preparation of larger, superstructured porphyrin assemblies.

## Experimental Section

**Synthesis of  $\beta$ ,*meso*-Linked Bisporphyrins 6 (Typical Procedure).** **5,10,15-Triphenyl-20-(5',10',15',20'-tetraphenylporphyrin-2'-yl)-porphyrin (6a).** A Schlenk flask filled with 5-bromo-10,15,20-triphenylporphyrin (**5a**, 164 mg, 266  $\mu$ mol, 1 equiv),  $\beta$ -borylated TPP **4a** (295 mg, 398  $\mu$ mol, 1.5 equiv), and Ba(OH)<sub>2</sub>·8H<sub>2</sub>O (839 mg, 2.66 mmol, 10 equiv) was evacuated and flushed with nitrogen three times. Toluene (50 mL) and deionized H<sub>2</sub>O (10 mL) were added, and the solution was degassed by a nitrogen stream in an ultrasonic bath for 15 min. Pd(PPh<sub>3</sub>)<sub>4</sub> (61.5 mg, 53.2  $\mu$ mol, 20 mol %) was added, and the resulting mixture was refluxed for 20 h with vigorous stirring. The crude mixture was cooled to room temperature and passed through a short plug of silica gel eluting with CH<sub>2</sub>Cl<sub>2</sub>. Concentration of the filtrate and purification of the resulting residue by column chromatography on silica gel using CH<sub>2</sub>Cl<sub>2</sub>/*n*-hexane (1:1, v/v) as the eluent afforded **6a** as a purple solid (199 mg, 173  $\mu$ mol, 65%);  $R_f$  = 0.14 (CH<sub>2</sub>Cl<sub>2</sub>/hexane, 1:1, v/v); mp (CH<sub>2</sub>Cl<sub>2</sub>/MeOH): > 300 °C; IR (ATR)  $\tilde{\nu}$  = 3313 (w), 3053 (m), 2920 (m), 2851 (w), 1595 (m), 1556 (w),

(74) This assumption is affirmed by the fact that, in the course of our investigations, RI-PBE-D/SV(P) calculations of a dimeric model system predicted the existence of two main tautomers (regarding the NH protons of the  $\beta$ -linked porphyrin macrocycle) in a ratio of 1:2.8 in the gas phase. Detailed investigations on this phenomenon are in progress.

1471 (m), 1439 (m), 1347 (m), 1173 (m), 1071 (m), 1001 (m), 979 (m), 962 (s), 796 (s)  $\text{cm}^{-1}$ ;  $^1\text{H}$  NMR (400 MHz,  $\text{CDCl}_3$ )  $\delta = -2.80$  (bs, 2H, NH),  $-2.34$  (bs, 2H, NH),  $4.05$  (app t,  $^{\text{app}}J(\text{H,H}) \approx 7.6$  Hz, 1H,  $p\text{-}20^{4'}$ -Ar-H),  $4.75$  (app t,  $^{\text{app}}J(\text{H,H}) \approx 7.6$  Hz, 1H,  $m\text{-}20^{3'}$ -Ar-H/1H,  $m\text{-}20^{5'}$ -Ar-H),  $6.89$  (app d,  $^{\text{app}}J(\text{H,H}) \approx 7.6$  Hz, 1H,  $o\text{-}20^{2'}$ -Ar-H/1H,  $o\text{-}20^{6'}$ -Ar-H),  $7.62\text{--}7.85$  (m, 18H, Ar-H),  $8.14\text{--}8.18$  (m, 2H, Ar-H),  $8.19\text{--}8.24$  (m, 3H, Ar-H/1H,  $\beta$ -pyrrole-H),  $8.29\text{--}8.36$  (m, 4H, Ar-H),  $8.37\text{--}8.42$  (m, 1H, Ar-H),  $8.44\text{--}8.49$  (m, 2H, Ar-H),  $8.59$  (d,  $^3J = 4.8$  Hz, 2H,  $\beta$ -pyrrole-H),  $8.63$  (d,  $^3J = 4.8$  Hz, 1H,  $\beta$ -pyrrole-H),  $8.66$  (d,  $^3J = 4.8$  Hz, 1H,  $\beta$ -pyrrole-H),  $8.83\text{--}8.89$  (m, 5H,  $\beta$ -pyrrole-H),  $8.90$  (d,  $^3J = 4.8$  Hz, 1H,  $\beta$ -pyrrole-H),  $8.98$  (d,  $^3J = 4.8$  Hz, 1H,  $\beta$ -pyrrole-H),  $9.01$  (d,  $^3J = 4.8$  Hz, 1H,  $\beta$ -pyrrole-H),  $9.69$  (s, 1H,  $3'\text{-}\beta$ -pyrrole-H) ppm;  $^{13}\text{C}$  NMR (100 MHz,  $\text{CDCl}_3$ ):  $\delta = 120.2$ ,  $120.4$  (two peaks),  $120.5$ ,  $122.2$ ,  $122.4$ ,  $124.1$ ,  $126.8$ ,  $126.9$  (two peaks),  $127.0$ ,  $127.7$ ,  $127.8$  (two peaks),  $127.9$ ,  $128.0$ ,  $132.2$ ,  $134.5$ ,  $134.6$ ,  $134.7$ ,  $134.8$  (two peaks),  $134.9$  (two peaks),  $139.1$ ,  $142.1$ ,  $142.3$ ,  $142.4$ ,  $142.6$  (two peaks) ppm; HRMS (ESI) calcd for  $\text{C}_{82}\text{H}_{54}\text{N}_8$  [ $\text{M}^+$ ] 1150.4466, found 1150.4466; UV-vis ( $\text{CH}_2\text{Cl}_2$ )  $\lambda_{\text{max}}$  (log  $\epsilon$ ) = 422 (5.72), 441 (5.73), 522 (4.79), 559 (4.31), 597 (4.15), 654 (3.61) nm.

**Synthesis of  $\beta$ ,Meso-Linked Triporphyrins 8 (Typical Procedure).** **5,15-Diphenyl-10,20-bis-(5',10',15',20'-tetraphenylporphyrin-2'-yl)porphyrin (8a).** A Schlenk flask filled with 5,15-dibromo-10,20-diphenylporphyrin (**7a**, 84 mg, 135  $\mu\text{mol}$ , 1 equiv),  $\beta$ -borylated TPP **4a** (250 mg, 338  $\mu\text{mol}$ , 2.5 equiv), and  $\text{Ba}(\text{OH})_2 \cdot 8\text{H}_2\text{O}$  (852 mg, 2.70 mmol, 20 equiv) was evacuated and flushed with nitrogen three times. Toluene (50 mL) and deionized  $\text{H}_2\text{O}$  (10 mL) were added, and the solution was degassed by a nitrogen stream in an ultrasonic bath for 15 min.  $\text{Pd}(\text{PPh}_3)_4$  (31.2 mg, 27.0  $\mu\text{mol}$ , 20 mol %) was added, and the resulting mixture was refluxed for 24 h with vigorous stirring. The crude mixture was cooled to room temperature and passed through a short plug of silica gel eluting with  $\text{CH}_2\text{Cl}_2$ . Concentration of the filtrate afforded **8a** as a mixture of diastereomers that were isolated in pure form after column chromatography on silica gel using  $n$ -hexane/ $\text{CH}_2\text{Cl}_2$  (1:1, v/v) as the eluent: The first eluting triporphyrin band yielded the *trans*-isomer *trans*-**8a** (purple solid, 118 mg, 70.2  $\mu\text{mol}$ , 52%) while the second eluting band contained the respective *cis*-isomer *cis*-**8a** (purple solid, 60.9 mg, 36.1  $\mu\text{mol}$ , 27%). Compound *trans*-**8a**:  $R_f = 0.19$  ( $\text{CH}_2\text{Cl}_2$ /hexane, 1:1, v/v); mp ( $\text{CH}_2\text{Cl}_2$ /MeOH)  $>300$  °C; IR (ATR)  $\tilde{\nu} = 3310$  (w), 3054 (m), 2922 (m), 1597 (m), 1559 (w), 1472 (m), 1439 (m), 1347 (m), 1244 (m), 1172 (m), 1072 (m), 1032 (m), 1001 (m), 979 (m), 962 (s), 793 (s)  $\text{cm}^{-1}$ ;  $^1\text{H}$  NMR (600 MHz,  $\text{CDCl}_3$ )  $\delta = -2.83$  (bs, 2H, "inner" NH),  $-2.33$  (bs, 4H, "outer" NH),  $4.00$  (app t,  $^{\text{app}}J(\text{H,H}) \approx 7.6$  Hz, 1H,  $p\text{-}20^{4'}$ -Ar-H/1H,  $p\text{-}20^{4''}$ -Ar-H),  $4.68$  (app t,  $^{\text{app}}J(\text{H,H}) \approx 7.4$  Hz, 1H,  $m\text{-}20^{3'}$ -Ar-H/1H,  $m\text{-}20^{5'}$ -Ar-H/1H,  $m\text{-}20^{3''}$ -Ar-H/1H,  $m\text{-}20^{5''}$ -Ar-H),  $6.86$  (app d,  $^{\text{app}}J(\text{H,H}) \approx 6.9$  Hz, 1H,  $o\text{-}20^{2'}$ -Ar-H/1H,  $o\text{-}20^{6'}$ -Ar-H/1H,  $o\text{-}20^{2''}$ -Ar-H/1H,  $o\text{-}20^{6''}$ -Ar-H),  $7.65\text{--}7.78$  (m, 18H, Ar-H),  $7.80\text{--}7.86$  (m, 6H, Ar-H),  $8.18\text{--}8.23$  (m, 4H, Ar-H/2H,  $\beta$ -pyrrole-H),  $8.24\text{--}8.28$  (m, 4H, Ar-H),  $8.30\text{--}8.35$  (m, 4H, Ar-H),  $8.49\text{--}8.53$  (m, 4H, Ar-H),  $8.59$  (d,  $^3J = 4.8$  Hz, 4H,  $\beta$ -pyrrole-H),  $8.63$  (d,  $^3J = 4.8$  Hz, 2H,  $\beta$ -pyrrole-H),  $8.66$  (d,  $^3J = 4.8$  Hz, 4H,  $\beta$ -pyrrole-H),  $8.86$  (d,  $^3J = 4.8$  Hz, 2H,  $\beta$ -pyrrole-H),  $8.90$  (d,  $^3J = 4.8$

Hz, 2H,  $\beta$ -pyrrole-H),  $8.98$  (d,  $^3J = 4.8$  Hz, 2H,  $\beta$ -pyrrole-H),  $9.03$  (d,  $^3J = 4.8$  Hz, 2H,  $\beta$ -pyrrole-H),  $9.83$  (s, 1H,  $3'\text{-}\beta$ -pyrrole-H/1H,  $3''\text{-}\beta$ -pyrrole-H) ppm;  $^{13}\text{C}$  NMR (150 MHz,  $\text{CDCl}_3$ )  $\delta = 116.1$ ,  $120.2$ ,  $120.3$ ,  $120.4$ ,  $120.7$ ,  $122.1$ ,  $122.2$  (two peaks),  $124.0$ ,  $126.6$  (two peaks),  $126.7$ ,  $126.8$ ,  $127.5$ ,  $127.6$ ,  $127.7$  (two peaks),  $127.8$ ,  $131.9$ ,  $134.5$  (two peaks),  $134.7$ ,  $134.8$ ,  $138.7$ ,  $142.0$ ,  $142.2$ ,  $142.4$ ,  $142.6$  ppm; HRMS (ESI) calcd for  $\text{C}_{120}\text{H}_{79}\text{N}_{12}$  [ $\text{M} + \text{H}^+$ ] 1686.6545, found 1686.6545; UV-vis ( $\text{CH}_2\text{Cl}_2$ )  $\lambda_{\text{max}}$  (log  $\epsilon$ ) = 419 (5.57), 455 (5.50), 522 (4.85), 574sh (4.43), 594 (4.49), 650 (4.10), 666 (4.10) nm. Compound *cis*-**8a**:  $R_f = 0.09$  ( $\text{CH}_2\text{Cl}_2$ /hexane, 1:1, v/v); mp ( $\text{CH}_2\text{Cl}_2$ /MeOH)  $>300$  °C; IR (ATR)  $\tilde{\nu} = 3315$  (w), 3054 (w), 2920 (m), 2850 (w), 1596 (m), 1559 (w), 1472 (m), 1440 (m), 1347 (m), 1259 (m), 1176 (m), 1071 (m), 1030 (w), 1001 (m), 979 (m), 962 (s), 796 (s)  $\text{cm}^{-1}$ ;  $^1\text{H}$  NMR (600 MHz,  $\text{CDCl}_3$ )  $\delta = -2.86$  (bs, 2H, "inner" NH),  $-2.29$  (bs, 4H, "outer" NH),  $4.85$  (app t,  $^{\text{app}}J(\text{H,H}) \approx 7.7$  Hz, 1H,  $p\text{-}20^{4'}$ -Ar-H/1H,  $p\text{-}20^{4''}$ -Ar-H),  $5.26\text{--}5.38$  (m, 1H,  $m\text{-}20^{3'}$ -Ar-H/1H,  $m\text{-}20^{5'}$ -Ar-H/1H,  $m\text{-}20^{3''}$ -Ar-H/1H,  $m\text{-}20^{5''}$ -Ar-H),  $7.24$  (app d,  $^{\text{app}}J(\text{H,H}) \approx 6.8$  Hz, 1H,  $o\text{-}20^{2'}$ -Ar-H/1H,  $o\text{-}20^{6'}$ -Ar-H/1H,  $o\text{-}20^{2''}$ -Ar-H/1H,  $o\text{-}20^{6''}$ -Ar-H),  $7.58\text{--}7.70$  (m, 10H, Ar-H),  $7.71\text{--}7.80$  (m, 8H, Ar-H),  $7.81\text{--}7.86$  (m, 6H, Ar-H),  $8.15$  (d,  $^3J = 7.4$  Hz, 2H, Ar-H),  $8.22\text{--}8.29$  (m, 4H, Ar-H),  $8.30\text{--}8.36$  (m, 4H, Ar-H),  $8.37\text{--}8.46$  (m, 6H, Ar-H/2H,  $\beta$ -pyrrole-H),  $8.58$  (d,  $^3J = 4.8$  Hz, 4H,  $\beta$ -pyrrole-H),  $8.64$  (d,  $^3J = 4.8$  Hz, 4H,  $\beta$ -pyrrole-H),  $8.73$  (d,  $^3J = 4.8$  Hz, 2H,  $\beta$ -pyrrole-H),  $8.90$  (d,  $^3J = 4.8$  Hz, 2H,  $\beta$ -pyrrole-H),  $8.93$  (d,  $^3J = 4.8$  Hz, 2H,  $\beta$ -pyrrole-H),  $8.98$  (d,  $^3J = 4.8$  Hz, 2H,  $\beta$ -pyrrole-H),  $9.01$  (d,  $^3J = 4.8$  Hz, 2H,  $\beta$ -pyrrole-H),  $9.61$  (s, 1H,  $3'\text{-}\beta$ -pyrrole-H/1H,  $3''\text{-}\beta$ -pyrrole-H) ppm;  $^{13}\text{C}$  NMR (150 MHz,  $\text{CDCl}_3$ )  $\delta = 116.1$ ,  $120.4$ ,  $120.5$ ,  $121.0$ ,  $122.1$ ,  $122.8$ ,  $124.3$ ,  $126.7$ ,  $126.8$ ,  $126.9$  (two peaks),  $127.0$ ,  $127.7$ ,  $127.9$  (two peaks),  $128.0$ ,  $133.0$ ,  $134.7$ ,  $134.8$ ,  $134.9$ ,  $139.8$ ,  $142.1$ ,  $142.4$ ,  $142.5$  (two peaks) ppm; HRMS (ESI) calcd for  $\text{C}_{120}\text{H}_{79}\text{N}_{12}$  [ $\text{M} + \text{H}^+$ ] 1686.6545, found 1686.6546; UV-vis ( $\text{CH}_2\text{Cl}_2$ )  $\lambda_{\text{max}}$  (log  $\epsilon$ ) = 419 (5.54), 454 (5.45), 521 (4.79), 574sh (4.36), 595 (4.52), 650 (4.01), 664 (4.02) nm.

**Acknowledgment.** The authors gratefully acknowledge Carina Grimmer and Dr. Sabine Horn for preparing several of the monomeric porphyrin precursors, and Dr. Matthias Grüne for carrying out the VT-NMR measurements. This work was supported by the Degussa-Stiftung, the Studienstiftung des deutschen Volkes e.V. (fellowships to D. C. G. Götz), and the Science Foundation Ireland (Research Professorship Award o4/RP1/B482 to MOS).

**Supporting Information Available:** General experimental details, all experimental procedures at full length, detailed 2D NMR correlations, copies of the  $^1\text{H}$ ,  $^{13}\text{C}$ , COSY, and ROESY NMR spectra, CD spectra, chromatographic conditions for the resolution of the atropisomers, and information concerning the computational methods. This material is available free of charge via the Internet at <http://pubs.acs.org>.